Cumulative particle production on proton and nucleus beams

V. K. Bondarev
Joint Institute for Nuclear Research, Dubna

Fiz. Élem. Chastits At. Yadra **28**, 13-88 (January–February 1997)

The experimental results from a systematic study of cumulative $\pi^{\pm}$, $K^{\pm}$, p, and d production in the inclusive process $B+A\rightarrow c+X$ are presented. The beam B was protons, deuterons, helium nuclei, or carbon nuclei with momentum per nucleon equal to 4.5 GeV/c. The A dependence of the cross sections was measured for these beams for fixed secondary-particle momentum equal to 0.5 GeV/c and emission angle $\vartheta=120°$. The fragmenting nuclei are D, He, ^{6}Li, ^{7}Li, C, Al, Si, Cu, ^{58}Ni, ^{64}Ni, ^{64}Zn, ^{114}Sn, ^{124}Sn, and Pb. The energy dependence of the $\pi^{\pm}$-meson, proton, and deuteron cross sections in the momentum range 0.3–0.7 GeV/c ($\vartheta=120°$) was measured for ^{58}Ni, ^{64}Ni, ^{64}Zn, ^{114}Sn, ^{124}Sn, and Pb nuclei using an 8.9 GeV/c proton beam. Details of the behavior of the cross sections were found in various nuclear fragmentation regions. The behavior of the exponent of the A dependence of the proton, deuteron, and pion cross sections as a function of the mass number of the nuclei in the primary beam was studied. The results are compared with the data available in the literature. Various models of cumulative particle production in interactions of hadrons and nuclei with nuclei at various beam energies are discussed. Tables of invariant differential cross sections are presented, along with the results of fitting the energy dependence of the cross sections in various representations.
 [S1063-7796(97)00201-5]

INTRODUCTION

Systematic studies of cumulative particle production, i.e., particle production which is forbidden by conservation laws in collisions of free nucleons, were first begun by Baldin.[1] They were discovered experimentally by the Stavinskiĭ group at the JINR synchrophasotron in the process D(10 GeV/c)+Cu$\rightarrow\pi^{-}(0°)+X$ (Ref. 2). Pions with energy considerably greater than the energy per nucleon of the deuteron were observed in that experiment. According to the limiting-fragmentation hypothesis of Yang,[3] in this experiment the source of high-energy pions is the acclerated deuterium nuclei, and the contribution of the target nucleus is insignificant. This idea was confirmed in subsequent experiments.

The first experimental indications of unusual phenomena in hadron–nucleus interactions were the results from elastic pd scattering of 660-MeV protons[4] and quasielastic deuteron knockout from light nuclei in a 675-MeV proton beam.[5] The data of both these studies clearly indicated that the collision was collective in nature, i.e., two or more nucleons could be found at short distances. The results of these studies served as the basis for the hypothesis that dense clusters of nucleons exist in nuclei for a short time. These are the nuclear-matter density fluctuations predicted by Blokhintsev.[6] Now they are referred to as fluctons or few-nucleon correlations.

The early stage of the study of cumulative processes during the period 1971–1982 is discussed in the reviews of Refs. 7–11. The physical basis for studies using relativistic nuclei is discussed in Ref. 7, where the scale-invariant behavior and the specific A dependence of the cross sections for the cumulative effect are obtained. A brief review is also given of the program of research using relativistic nuclei at the JINR High Energy Laboratory. The experimental data obtained by various groups and the characteristic features of cumulative particle production are summarized in Ref. 8. The physical nature of fluctons as multiquark configurations in nuclei and the existence of fluctons in the bag model are discussed in Ref. 9. The model of few-nucleon correlations and its application to hadron–nucleus and nucleus–nucleus collisions are described in Ref. 10. Various models of cumulative particle production are compared with the experimental data in Ref. 11. The results of studies carried out in the last decade are noteworthy for the improved accuracy of the experimental data and the development of better theoretical models.

At present there is a great deal of experimental data on cumulative particle production. In most cases the experiments were designed such that cumulative particles are recorded in the angular range 90°–180° (the backward hemisphere) in inclusive processes $B+A\rightarrow c+\ldots$. In this case, fragmenting target nuclei are the source of cumulative particles. The most complete studies are those which have been performed in proton beams in the energy range 1–400 GeV. In addition, there are data on the cumulative production of protons on γ, ν, $\bar{\nu}$, $\pi^{\pm}$, K^{-}, and $\bar{p}$ beams, and fragmentary data for beams of D, He, and C nuclei. The spectrum of cumulative particles includes $\pi^{\pm}$ mesons, $K^{\pm}$ mesons, Λ, p, n, $\bar{p}$, and the nuclear fragments d, t, ^{3}He, and ^{4}He. Fragmenting nuclei in a wide range from deuterium to uranium have been studied, including isotopically separated lithium, boron, nickel, zinc, tin, samarium, and tungsten nuclei.

Let us briefly discuss the typical features and the main results obtained in studies of cumulative processes and introduce the needed definitions.

BASIC REGULARITIES IN CUMULATIVE PARTICLE PRODUCTION

Energy dependence. The traditional representation of the results on the energy dependence of the cross sections essentially reduces to the following expressions:

$$\frac{1}{A} E \frac{d\sigma}{d\mathbf{p}} = B_T \exp\left(-\frac{T}{T_0}\right), \quad (1)$$

$$\frac{1}{A} E \frac{d\sigma}{d\mathbf{p}} = B_x \exp\left(-\frac{x}{x_0}\right), \quad (2)$$

$$\frac{1}{A} E \frac{d\sigma}{d\mathbf{p}} = B_\alpha \exp\left(-\frac{\alpha}{\alpha_0}\right). \quad (3)$$

Here, E, $\mathbf{p}$, and A are the energy, the secondary-particle momentum, and the mass number of the fragmenting nucleus, T is the kinetic energy of the observed particle, and T_0, x_0, and α_0 are the slope parameters of the spectra. The scaling variable x, as in deep-inelastic scattering, is the Bjorken variable, modified for the case of moderate initial energy.[8] Writing the inclusive process as

$$\mathrm{I}+\mathrm{II}\to 1+\cdots, \quad (4)$$

where the symbols refer to the primary beams, the fragmenting nuclei, and the secondary particles, we obtain an expression for the variable x:

$$x=\frac{(P_\mathrm{I}P_1)+M_\mathrm{I}M_1+(M_2^2-M_1^2)/2}{(P_\mathrm{I}P_\mathrm{II})-(P_1P_\mathrm{II})-M_\mathrm{I}M_\mathrm{II}-M_2M_\mathrm{II}}. \quad (5)$$

Here P_I and P_II are the 4-momenta per nucleon of the projectile and the target, respectively; P_1 is the 4-momentum of the measured particle; M_I, M_II, and M_1 are the corresponding masses; M_2 is the additional particle mass needed to satisfy the conservation laws (in the calculations it is assumed that $M_{2\pi}=0$, $M_{2K}=M_\Lambda-M_p$, $M_{2p}=-M_p$, and so on). In contrast to the Feynman and Bjorken scaling variables, x varies from 0 to A (A is the nuclear mass number), and in a first approximation it corresponds to the number of nucleons needed to produce a cumulative particle with given characteristics (momentum, mass, and so on).

The light-front variable α is given by

$$\alpha=\frac{E-P\cos\vartheta}{M_n}, \quad (6)$$

where E, P, and ϑ are respectively the particle energy, momentum, and emission angle, and M_n is the nucleon mass. We immediately note that the variable x that we use, the Feynman and Bjorken variables, and α all coincide at high initial energies.

For fixed emission angles the energy spectra of the various particles are similar for different nuclei. The cross sections depend exponentially on the kinetic energy of the cumulative particles or on the other variables, and the slope parameters of the spectra in various representations are different for light and heavy nuclei. Already in the early studies of cumulative particle production[12,13] it was shown that the slope parameter T_0 has the same value for different nuclei (C, Al, Cu, Pb), and is approximately 60 MeV for pions at an emission angle of 180°. In later studies,[8,14,15] where cumulative production was studied throughout the backward hemisphere and the cumulative-particle spectrum included kaons, protons, and baryon fragments, it was shown that there is a general regularity in the behavior of the cross sections, characterized by a single slope parameter $x_0\simeq 0.14$ for intermediate and heavy nuclei. The ITEP–Pennsylvania experiments using a 400-GeV proton beam played an important role in establishing the scale-invariant behavior of the cumulative-production cross sections.[16–18] It was concluded from the results of Refs. 8, 12, 13, and 14–18 that limiting nuclear fragmentation as a function of the scaling variable x is realized in the range of initial energies 4–400 GeV. Here the values of x varied from 0.35 to 3.5, depending on the characteristics of the observed particles (the mass, momentum, emission angle, and initial energy). The cross sections for pions change by nine orders of magnitude in this range of x.

In recent years experimental data have been obtained in this range of primary proton energies. Data for 10 GeV are given in Refs. 19–22, and data at 15–65 GeV are given in Refs. 23 and 24. Cumulative proton production on 40-GeV/c π^-, K^-, and $\bar{p}$ beams was studied in Ref. 25. These studies confirm the characteristic features of cumulative particle production and, naturally, contribute to a deeper understanding of these processes.

Since the properties of cumulative particles turned out to be rather conservative for different energies and types of primary beam and fragmenting nucleus, this was reflected in the empirically established facts. The approximate independence of the shape of the proton spectra, normalized to the total inelastic cross section, of the energy and type of primary particle, and the hierarchy of attainment of scaling behavior with increasing mass number of the fragmenting nucleus are known as the phenomenological hypothesis of nuclear scaling.[26,27] The universality of the shapes of the p, $\bar{p}$, $\pi^\pm$, and $K^\pm$ spectra in any of the scaling variables is referred to as superscaling by the authors of Ref. 22.

Analysis of cumulative production processes led to the concept of the quark–parton structure function,[28] which characterizes the probability for a nuclear constituent to have momentum corresponding to that of a group of nucleons. The nuclear constituent in question is understood as a quark; a group of nucleons in a small volume is transformed into a multiquark configuration. The interaction between hadrons (and nuclei) arises as a result of individual collisions of the quarks of the fragmenting nucleus with the quarks and gluons of the target. A spectator quark not involved in a collision carries a fraction of the momentum of the fragmenting hadron. The hadronization of a quark is considered to be a soft process, and the distribution of hadron–fragments is assumed to correspond to the distribution of the spectator quark.

The A dependence. The very first experiments to study the cumulative effect demonstrated that the cross section for cumulative production of pions is proportional to the nuclear mass number A.[13] This came to be referred to as enhanced A dependence of the cross sections, because the typical dependence of the pion production cross section in hadron–nucleus interactions is characterized by exponent $n\simeq 2/3$. Further studies[16,29,30] revealed that the exponent n is greater than unity in the case of cumulative proton production ($n\simeq 1.3$), and is even greater for baryon systems like d, t, and so on. In addition, it was found that the cross section for cumulative proton production is independent of the number

of neutrons for fixed nuclear charge Z (the isotopic effect). The quoted values of n pertain to the region of intermediate and heavy nuclei. If we consider the A dependence of the cross sections normalized to the nuclear mass numbers, we find that it is characterized by a sharp increase of the cross sections in the region of light nuclei, after which the cross sections flatten out as A increases. The constant value is reached in different regions of nuclei for different particles. For example, for pions this regime sets in at $A \simeq 30$, and for protons and baryon fragments it sets in at $A \simeq 100$.

If the dependence of the cross sections on the mass number A is described by a power law, $E(d\sigma/d\mathbf{p}) \sim A^n$, then for protons, deuterons, and tritium the exponent n is 1.3, 1.6, and 2, respectively. Since the production cross sections are independent of the neutron excess, the Z dependence of the cross sections is more regular. This regularity in the Z dependence[30] is manifested for both light and heavy nuclei. For example, for protons and deuterons the exponent n is respectively 2 and 2.6 for nuclei in the range from Li to Al. In the range from Al to U the values are 1.5 and 1.7 for protons and deuterons, respectively. This dependence has been measured for 20 nuclei, including isotopically enriched ones.

The excess of the exponent n over unity is usually associated with the rescattering of created particles on intranuclear nucleons, the final-state interaction, and other secondary processes. Another viewpoint is that, as in the case of cumulative pion production, the processes producing protons and other fragments are equally probable throughout the nuclear volume, but the boundary layer can have an effect. If the primary interaction occurs near the nuclear surface, the nuclear medium is insufficient for the production of a massive fragment. Then it is not the entire volume of the nucleus which is effectively involved, but the volume decreased by the thickness of the surface layer. Here it is obvious that the thickness of the surface layer must be correlated with the fragment mass. A quantitative estimate is made assuming that the cross sections for fragment production behave as

$$E\frac{d\sigma}{d\mathbf{p}} \sim (r_0 A^{1/3} - \rho)^3. \tag{7}$$

Here $r_0 A^{1/3}$ is the nuclear radius, where $r_0 = 1.2$ F. The quantity ρ can be associated with the size of the fragment-emission region. Introducing the parameter $\xi = \rho/r_0$ and using the ratio of the cross sections on various nuclei to that at the mass number of lead, the expression

$$\frac{E\frac{d\sigma}{d\mathbf{p}}(A)A_{\mathrm{Pb}}}{AE\frac{d\sigma}{d\mathbf{p}}(A_{\mathrm{Pb}})} = \left(\frac{1-\xi A^{-1/3}}{1-\xi A_{\mathrm{Pb}}^{-1/3}}\right)^3 \tag{8}$$

can be used to find the parameter ξ. The values of ξ thus obtained are $\xi_p = 0.9$, $\xi_d = 1.6$, and $\xi_t = 2$. It can be seen that there is actually a correlation with the fragment mass. The inclusion of the parameter ξ leads for these fragments to a volume-type A dependence in a wide range of cumulative-particle momenta and emission angles. A detailed procedure for studying the A dependence on the basis of these representations can be found in Ref. 15.

In Ref. 19 the volume nature of the A dependence of the cross sections was associated with the effect of the right-hand kinematical limit of the process $pA \to p(\pi)X$. Denoting the invariant differential cross section as $f(x)$, we can write $f(x) = f_0(x)(1 - x/A)^n$, where n is a parameter. This expression satisfactorily describes the data with the parameter $n = 8 \pm 1$ for protons and $n = 7 \pm 1$ for pions. The function f_0 is approximated well by the expression $C \exp(-x/x_0)$ for $x_0 = 0.135 \pm 0.001$ for protons and $x_0 = 0.139 \pm 0.002$ for pions. The values of f_0 are close for the data at initial energies of 10 and 400 GeV, and identical for different nuclei.

The angular dependence. The spectra of cumulative particles at various angles (backward hemisphere) have been measured in pA and dA interactions in Refs. 14 and 15. The slope parameter T_0 of the spectra varies as a function of the particle emission angle. It increases by about a factor of 1.5 in the angular range 180°–90°. Measurements of the angular dependence of the cross sections at fixed particle momenta showed that the behavior scales on different nuclei, in particular, for helium and lead nuclei,[8] which may indicate that rescattering processes are absent or relatively unimportant. The dependences of the proton and deuteron cross sections on the ^{6}Li nucleus also demonstrate scaling (the proton and deuteron momenta are 0.7 GeV/c). The angular dependence of the cross sections in the pA interaction has a clearly expressed structure for emission angles in the range 150°–180°, in particular, there is a peak in the backward direction. The irregularities in this angular range have also been studied in Ref. 31. The behavior of the cross sections is different in the case of the dA interaction. In both pA and dA interactions the invariant cross sections for cumulative-particle production do not depend linearly on $\cos\vartheta$ in the range of emission angles 180°–90°. The angular dependence of the cross sections for protons and light fragments was analyzed in Ref. 32 for pA interactions at a proton energy of 400 GeV.

The availability of data at different emission angles makes it possible to study the $p_\perp^2$ dependence of the cross sections. In particular, the following approximation has been found for pions:[14]

$$\varphi(p_\perp^2) = 0.9 \exp(-2{,}7p_\perp^2) + 0.1. \tag{9}$$

Taking into account the $p_\perp^2$ dependence, the pion data are represented by a single slope parameter in the angular range 90°–180°.

THE EXPERIMENTAL CONDITIONS

In spite of the diversity of primary beams, the data on cumulative particle production on nuclear beams are fragmentary. The experimental facilities of the High Energy Physics Laboratory at the JINR allow the gaps to be filled by systematic and detailed studies performed using the nuclear and proton beams of the synchrophasotron. In the experimental program using beams of p, D, α-particles, and C nuclei with momentum per nucleon equal to 4.5 GeV/c, the

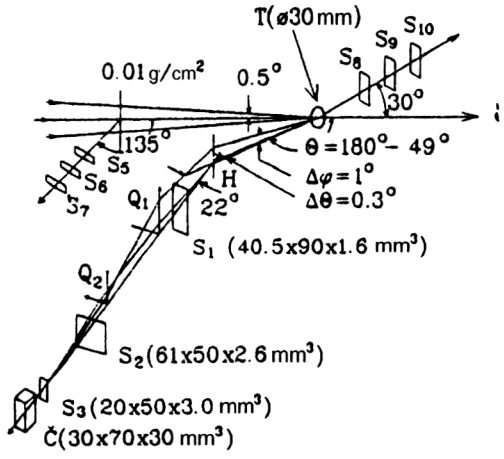

FIG. 1. Schematic view of the DISK-2 installation.

emphasis was on the detailed study of the A dependence of the cross sections, because it is the most interesting aspect of cumulative processes. The energy spectra were measured using an 8.9-GeV/c proton beam on isotopes of nickel, zinc, tin, and lead (with the natural mixture of isotopes). In all cases cumulative $\pi^{\pm}$, $K^{\pm}$, p, and d particles were recorded at the angle $\vartheta = 120°$. The data which are most reliable statistically were obtained for pions, protons, and deuterons. The following target nuclei were used in the experiments: D, He, ^{6}Li, ^{7}Li, C, Al, Si, Cu, ^{58}Ni, ^{64}Ni, ^{64}Zn, ^{114}Sn, ^{124}Sn, and Pb.

The experiment was performed using the DISK-2 setup, consisting of a time-of-flight spectrometer combined with magnetic analysis of the secondary particles in momentum. The setup is shown schematically in Fig. 1. The primary beam of accelerated particles is transported through a vacuum duct and focused by a magnetic optical system on the target (T) with an image spread of $\simeq 7$ mm. The secondary particles (target fragments) are momentum-analyzed by a sector magnet H (2SP94), pass through the counter S_1, and are focused by the doublet of quadrupole lenses Q_1 and Q_2 (1ML15 and 2ML15) on the counter S_4. They also pass through the counters S_2 and S_3, the Čerenkov counters C_t and C_b based on solid radiators, and the gas Čerenkov counter C_g. The counters S_4, C_t, and C_b are constructed as a single unit and are not shown in Fig. 1. The magnetic optical channel (H, Q_1, and Q_2) and the secondary-particle counters are located on two connected movable ribs with common rotation axis passing through the center of the target, located at the primary-beam focus. The channel is rotated remotely with an accuracy of 0.1° in the range of azimuthal angles 49°–180° (the angles 49°–90° for restricted size of the measuring area are reached by rotating the magnet H on a special platform about its axis by 180° and then reconnecting the ribs). The range of momenta recorded by the setup is 0.15–1.6 GeV/c for singly charged particles. The setup allows the following particles to be recorded simultaneously:

$$\pi^{\pm}, K^{\pm}, p, \bar{p}, d, t, {}^{3}\mathrm{He}, {}^{4}\mathrm{He}.$$

Two types of target were used in the experiments. The solid targets had a diameter of 30 mm and a thickness of 0.1–8 g/cm^2. The cryogenic targets of diameter 50 mm had dimension along the beam equal to 50 and 140 mm. Both types of target were mounted on a common housing, which could be moved in the vertical and horizontal directions. The target was placed in the beam remotely and controlled by a television system with a fluorescent screen. The primary beam was monitored by a telescope of counters S_5, S_6, and S_7 located at an angle of 135° relative to the direction of the primary beam (the monitor M_p) at a distance of 3 m from the target. The telescope M_p records particles produced in the interaction of the primary beam with the damper of the vacuum duct (mylar). The telescope of counters S_8, S_9, and S_{10} (the monitor M_π) is directed toward the target and serves to control the beam spill. The value and constancy of the ratio M_p/M_π throughout the spill cycle indicate complete passage of the primary-beam particles through the target. The calibration of the telescope M_p is based on measurement of the induced activity in the reaction $^{12}\mathrm{C}(p,pn)^{11}\mathrm{C}$. For this purpose, a plastic scintillator is bombarded at the focus of the primary beam, and the induced activity is measured using a specially designed setup.

The counter S_1 is located near the magnet H at a distance of 2.4 m from the target. The distance between counters S_1 and S_3 is 3.8 m, and that between S_2 and S_3 is 0.97 m. XP1021 photomultipliers are used in counters S_1–S_4, and their operating mode is chosen so as to obtain the best time resolution (± 50 psec) for linear dependence of the output charge signal on the number of photoelectrons. The Čerenkov counters C_t and C_b have radiators of polyethylmethacrylate of special purity, glued onto 56DVP photomultipliers. FEU-87 photomultipliers and scintillators of dimensions $50\times 10\times 0.8$ mm^3 are used in the monitoring telescopes M_p and M_π. The magnetic spectrometer was calibrated by the current-carrying wire method,[33] and allowed determination of the central particle pulse as a function of the current in the magnet or of the magnetic-field strength according to a Hall probe. The momentum resolution $\Delta p/p$ of the spectrometer is 8%. The acceptance of the setup is 3.4×10^{-5} sr, and the absolute normalization of the cross sections is 10–15% (the last number pertains to a beam of carbon nuclei).

Secondary particles separated by the magnet H according to their charge and momentum pass through the counters S_1–S_4 and the Čerenkov counters and are identified by measuring the following characteristics:

- The particle time of flight on the baseline S_1–S_3 (t_1).
- The particle time of flight on the baseline S_2–S_3 (t_2).
- The ionization losses of particles in the scintillators S_2, S_3, and S_4.
- The intensities of Čerenkov radiation of particles in the radiators of counters C_t and C_b.

The algorithm of the τ criteria provides an efficient method of isolating useful events. Using the linear relation between the particle times of flight on the two baselines t_1 and t_2, the τ coordinate can be determined from the expression

$$\tau_{t2} = t_1 - 2t_2 + 260.$$

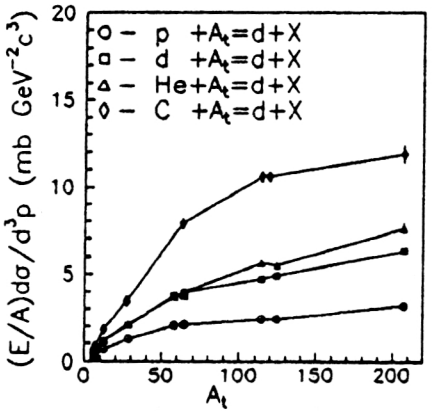

FIG. 2. A dependence of the deuteron cross sections on various beams.

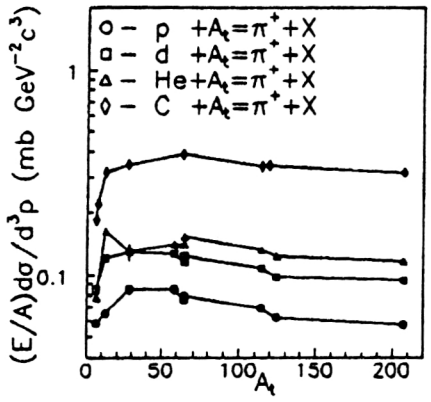

FIG. 4. A dependence of the π^+ cross sections on various beams.

In this coordinate, events not associated with random signals in the counters have a distribution independent of the velocity of the detected particles, and their distribution in τ_{t2} has a single maximum. Specification of the limits for the corresponding useful events leads to suppression of background events by more than a factor of 20. Similarly, using the criterion

$$\tau_{\Delta E3}=t_1-2.6t_2+150,$$

we obtain a distribution in which all events not associated with random ones are separated in charge and, in a first approximation, are not separated in velocity. In addition to the charge separation, measurement of the ionization losses raises the reliability of the particle identification. The setup operates on-line with a computer.

The set of values t_1, t_2, Δ_{E2}, Δ_{E3}, Δ_{E4}, I_{C_t}, and I_{C_b} forms the event space. A region in event space is specified by the condition that the event coordinates be observed simultaneously within given ranges of each coordinate. The multidimensional-analysis program allows events in different multidimensional regions to be distinguished and the one- and two-dimensional projections of the events contained in these regions to be constructed on the coordinate axes of the event space during the data analysis. Analysis of the resulting distributions makes it possible to evaluate the number of events of a particular type, the statistical characteristics of the spectra, and the contribution of random coincidences for high charge loads in the detector. In addition, the multidimensional analysis for each type of particle produces a bank of integrated characteristics of useful events. This contains, for each type of particle, information about the number of events, the effectiveness of the limits in each of the coordinates used, and the average amplitude of the event distribution in each coordinate. The programs feeding information into the bank are optimized in time, and allow all the information for all types of secondary particle recorded simultaneously to be processed between accelerator cycles. After each series of measurements the information contained in the bank is written into a file of final results located on a memory disk. The setup and procedure for calculating the cross sections from the measured quantities are described in detail in Refs. 34–36.

The targets of separated isotopes used in the experiments had the following enrichments (in percent relative to the main isotope): ^{6}Li (90.3), ^{7}Li (99), ^{58}Ni (99.7), ^{64}Ni (93.1), ^{64}Zn (98.7), ^{114}Sn (92), and ^{124}Sn (97.2). The correction associated with the difference from 100% enrichment is $\simeq 1\%$ on the average.

THE EXPERIMENTAL RESULTS

Proton–nucleus and nucleus–nucleus interactions. In Figs. 2–5 we give the data on the A dependence of the cross

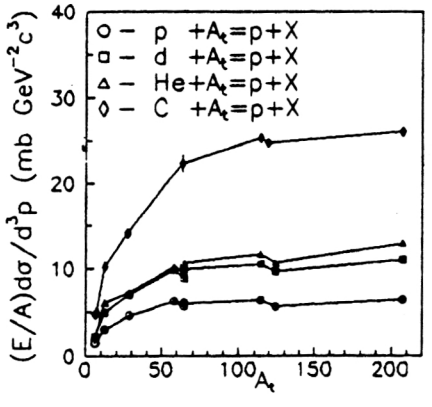

FIG. 3. A dependence of the proton cross sections on various beams.

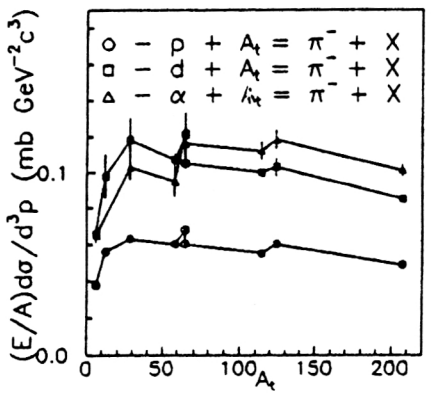

FIG. 5. A dependence of the π^- cross sections on various beams.

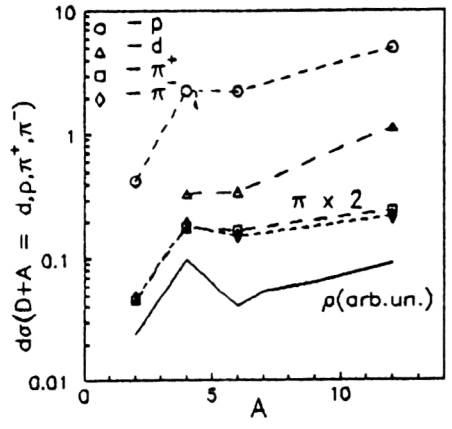

FIG. 6. A dependence of the cross sections for cumulative particles in the process $D+A \to c+\ldots$ ($\vartheta = 120°$).

sections for deuterons, protons, and positive and negative pions on proton, deuteron, He, and C beams.[37] As noted above, the cross sections are seen to increase sharply in the region of light nuclei, and to flatten out as the mass number A increases. This behavior is characteristic of all the beams used. It should be noted that the cross sections on deuterium and helium beams are close in magnitude, while the cross sections for different particles are similar. Another feature can be seen from the figures for isotopes of nickel, zinc, and tin. There are irregularities in the behavior of the cross sections which are manifested specifically for protons and π^+ and π^- mesons.

The behavior of the cross sections as a function of A is similar to that of such nuclear characteristics as the density, binding energy, and charge radii. These properties of nuclei are well known (see, for example, Ref. 38). With these properties in mind, let us consider light and heavy nuclei separately. The data on the A dependence of the cross sections for fragmenting nuclei from deuterium to carbon are shown in Fig. 6 on a magnified scale.[39] The lines on the graph connect the points. The solid line shows the behavior of the nuclear density calculated from

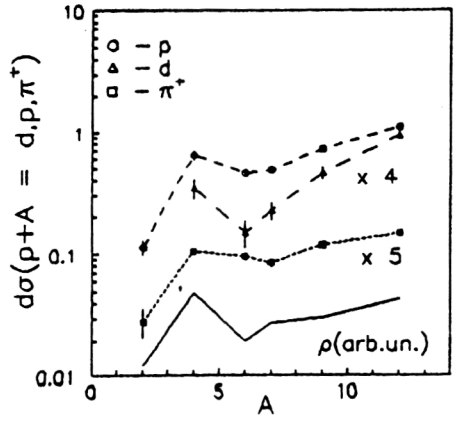

FIG. 7. A dependence of the cross sections for cumulative particles in the process $p+A \to c+\ldots$ ($\vartheta = 180°$).

TABLE I. π^+/π^- cross-section ratios for various beams.

A_t	$p+A_t$	$D+A_t$	$^4He+A_t$
^6Li	1.21±0.03	1.12±0.06	1.05±0.07
Pb	0.96±0.03	0.99±0.04	1.05±0.03

$$\rho(A) = \frac{A}{\frac{4}{3}\pi\left(\frac{5}{3}\langle r^2\rangle\right)^{3/2}}. \tag{10}$$

The values of the rms nuclear radii $\langle r^2\rangle$ were taken from Ref. 40. It is quite obvious that the behavior of the cross sections (Fig. 6) is correlated with the behavior of the nuclear density. A quantitative estimate can be obtained by comparing the density ratios with the cross-section ratios. For example, the increase of the density by a factor of 4.2 in going from deuterium to helium corresponds to cross-section ratios of 5.38±0.22, 3.90±0.13, and 3.86±0.13, respectively, for protons and π^+ and π^- mesons. Meanwhile, the decrease of the density by a factor of 2.5 in going from helium to lithium corresponds to the cross sections being equal for all particles. The passage from lithium to carbon again reveals a correlation: the ratio of the densities of carbon and lithium, equal to 2.25, corresponds to the cross-section ratios 2.22±0.06 (p), 3.26±0.09 (d), 1.43±0.04 (π^+), and 1.42±0.17 (π^-). We see from these numerical values that there really is a correlation between the cross sections and the density. In Fig. 7 we show the data for primary protons with momentum 8.9 GeV/c and emission angle 180°, taken from Refs. 14 and 15. The behavior of the cross sections here is the same as in Fig. 6, and even for nuclei in the range ^{4}He–^{6}Li the behavior is similar, with the possible exception of the deuteron data. Therefore, the studied region of light nuclei indicates that the cross sections for cumulative particles are correlated with the nuclear density, which varies maximally for these nuclei. This correlation is manifested in beams of protons and nuclei, is independent of the emission angle and type of particle, and in all probability has a quite general nature.

Using the data of Ref. 41, where the numerical values of the invariant differential cross sections for the particles studied here are given, and of Ref. 42, let us give a number of relations which are obeyed by the processes under study. One of the interesting characteristics in cumulative particle production is the π^+/π^- cross-section ratio. In Table I we give these ratios on various beams for light (^{6}Li) and heavy (Pb) nuclei.

We see from the data of Table I that these ratios are nearly equal to unity in isotopically conjugate processes, which is natural, and they are unity for the lead nucleus, which has a large neutron excess. The π^-/π^+ cross-section

TABLE II. p/π^+ cross-section ratios for various beams.

A_t	$p+A_t$	$D+A_t$	$^4He+A_t$	$C+A_t$
^6Li	25.3±0.7	26.4±0.8	27.6±1.2	26.0±0.9
Pb	113±3	117±5	110±5	82±4

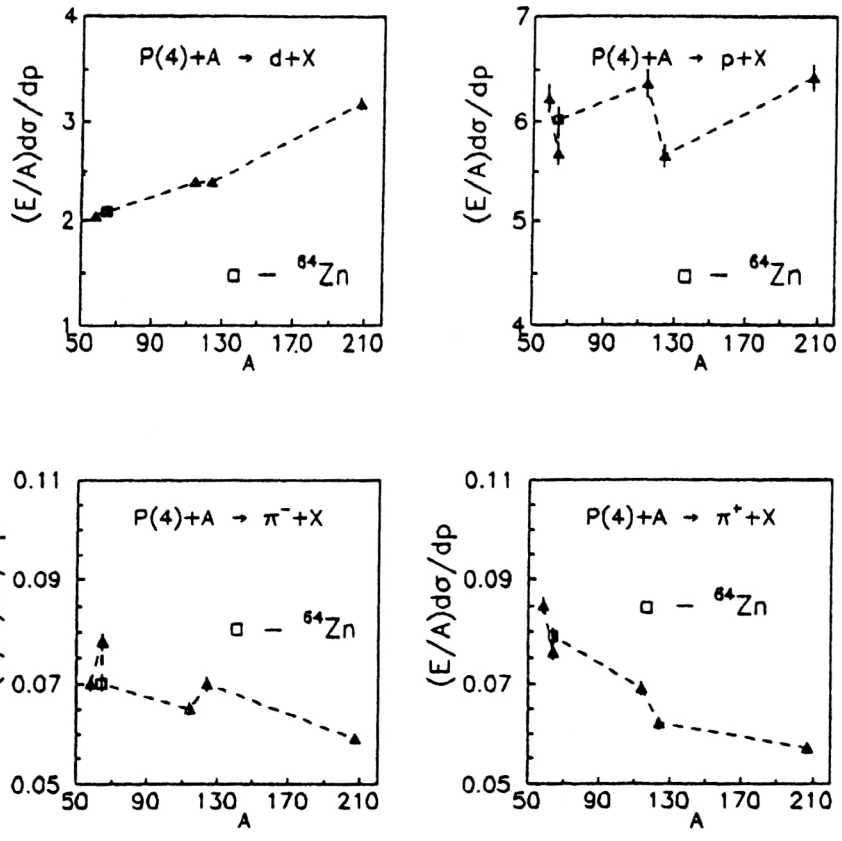

FIG. 8. A dependence of the deuteron, proton, and pion cross sections for a proton beam.

ratio in the elementary processes $p+p\to\pi^-$ and $p+p\to\pi^+$ is $\simeq 0.25$. The same ratio in the process $p+\mathrm{D}\to\pi$ is $\simeq 1$. This question was studied specially in Ref. 43. It is interesting to follow the ratios of the proton and π^+ cross sections for the case of nuclear beams. For comparison, we have again chosen lithium and lead nuclei. The results are given in Table II. From the data of this table we conclude that the p/π^+ cross-section ratios are constant for all beams, that they differ by about a factor of 4 on lead and lithium, and that the ratio decreases significantly on carbon. The decrease of the p/π^+ cross-section ratio in the process C+Pb may be associated with suppression of the proton yield due to screening by the incident carbon nucleus. The possible manifestation of screening in nucleus–nucleus interactions was pointed out in Ref. 44.

Let us turn to the regions of intermediate and heavy nuclei. In these regions the density is approximately constant, but the charge density varies. We first studied the correlations between the cross sections and the nuclear charge density in Ref. 37. Experimental indications of this possibility had been noticed considerably earlier,[29,30] but the insufficient statistical reliability of the data did not allow any definite conclusions to be drawn at that time.

Let us consider the available data.[37,39] They are shown in Fig. 8 (primary protons), Fig. 9 (primary deuterons), and Fig. 10 (helium nuclei). The irregular behavior of the cross sections for all particles and primary beams is clearly seen for the scale used in these figures. This irregularity appears in isotopically enriched nickel, zinc, and tin nuclei. We noticed the effect earlier,[29] and it has become known as the isotopic effect. The irregularity is that the cross section for cumulative proton production is independent of the neutron excess in the nuclei. The isotopic effect was later confirmed in Ref. 45 using 7.5-GeV/c proton beams and 5-GeV/c π^- beams, and the isotonic effect was discovered. This is the independence of the neutron production cross section of the proton excess. Later,[46] we showed that the cross sections are independent of the neutron excess for π^+ and K^+ mesons. The recent data (see the figures for π^+, π^-, and p) allow us to conclude that the cross sections for positively charged particles are sensitive to the proton content of the fragmenting nucleus, while those for negatively charged particles are sensitive to the neutron content. The quantitative behavior of the cross sections on isotopically enriched targets is seen from Table III, which lists the cross-section ratios for the particles and beams studied.

From Table III we immediately see the following:

- The cross-section ratios on nuclei with the same charge and different neutron content (^{64}Ni/^{58}Ni, ^{124}Sn/^{114}Sn) are equal to unity for positively charged particles within the experimental error.
- The cross-section ratios on the same nuclei for negatively charged particles are greater than unity and follow the neutron excess of the nuclei.
- The cross-section ratios on nuclei with different charges (^{64}Zn/^{64}Ni) are greater than unity for positively charged particles and close to or less than unity for negatively charged ones.
- The scale of variation of the cross sections lies within the limits of the relative proton and neutron content in the

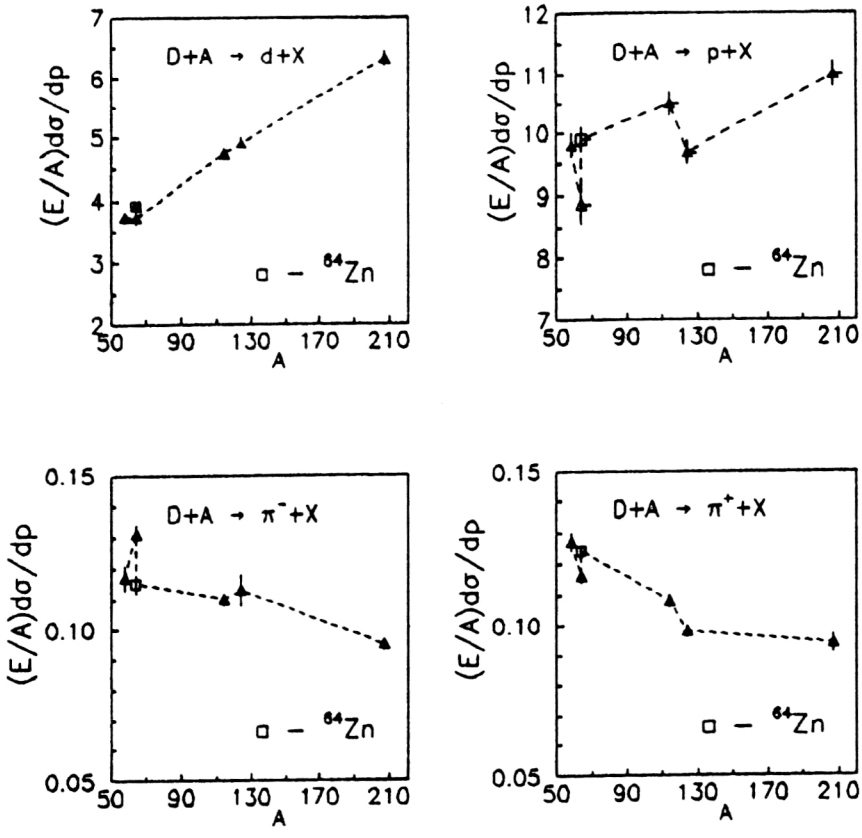

FIG. 9. *A* dependence of the deuteron, proton, and pion cross sections for a deuteron beam.

nuclei. This is a new and unexpected result for hadron–nucleus and nucleus–nucleus interactions in general and for cumulative processes in particular, especially because the π^+ and π^- cross sections are approximately equal for the

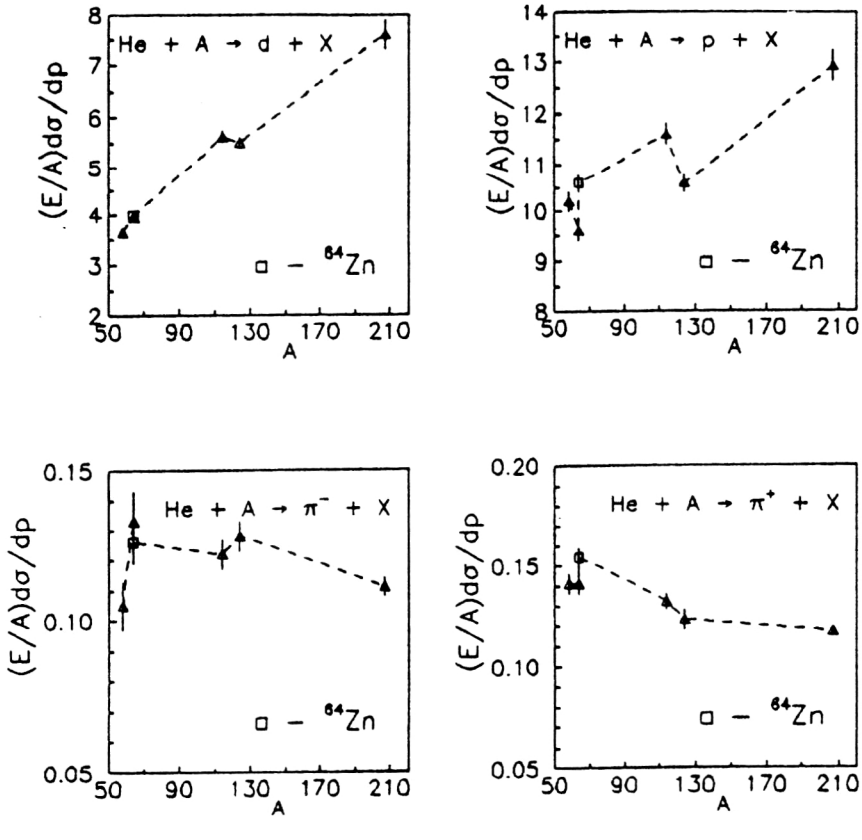

FIG. 10. *A* dependence of the deuteron, proton, and pion cross sections for a beam of He nuclei.

TABLE III. Cross-section ratios (not normalized to A) in various processes.

Process	^{64}Ni/^{58}Ni	^{124}Sn/^{114}Sn	^{64}Zn/^{64}Ni
p	1.00±0.03	0.97±0.03	1.06±0.03
$p+A\to\pi^+$	0.98±0.03	0.98±0.03	1.04±0.03
π^-	1.22±0.03	1.17±0.03	0.90±0.03
p	0.99±0.04	1.00±0.03	1.12±0.04
$D+A\to\pi^+$	1.00±0.03	0.99±0.03	1.07±0.02
π^-	1.24±0.06	1.12±0.05	0.88±0.03
p	1.04±0.03	0.99±0.03	1.10±0.03
^{4}He$+A\to\pi^+$	1.10±0.05	1.01±0.05	1.09±0.05
π^-	1.40±0.12	1.14±0.06	0.95±0.09

lead nucleus (the ratio of the number of neutrons to the number of protons is $N/Z=1.5$). This has been well known for a long time.

For the sake of comparison, we recall that the relative neutron content in isotopes of nickel and tin is 1.2 and 1.16, respectively. The ratio of the charges of ^{64}Zn and ^{64}Ni is 1.07.

The available experimental data for proton and nucleus beams make it possible to study the A dependence of the cross sections on the mass number of the primary beams directly. For this we determined the exponents n in the A dependence of the cross sections for pions, protons, and deuterons for each of the beams. The exponent n was found from the expression

$$n=\frac{\ln\left[E\frac{d\sigma}{d\mathbf{p}}(A_1)/E\frac{d\sigma}{d\mathbf{p}}(A_2)\right]}{\ln(A_1/A_2)}$$

The nuclei A_1 and A_2 were respectively taken to be Pb and Al. The numerical values of the exponent n are given in Table IV.

In Fig. 11 we show the dependence of n on the type of beam. The data of Table IV and Fig. 11 show that the A dependences of the cross sections for various beams are similar for pions, protons, and deuterons. The values of n become practically constant (a different constant for each particle) beginning with beams of helium nuclei.

PROTON–NUCLEUS INTERACTIONS USING 8.9-GeV/c BEAMS

The A dependence. The results obtained in studies with proton and nucleus beams using isotopically enriched targets stimulated interest in the more detailed study of this region of nuclei. Accordingly, measurements were made of the A dependence of the cross sections for cumulative $\pi^\pm$, $K^\pm$, p, and d production (momentum 0.5 GeV/c, $\vartheta=120°$) in an

TABLE IV. Values of the exponents n in various processes.

Process	d	p	π^+	π^-
$p+A$	1.45±0.02	1.16±0.01	0.80±0.01	0.84±0.02
D$+A$	1.56±0.02	1.23±0.02	0.84±0.02	0.85±0.11
^{4}He$+A$	1.64±0.02	1.29±0.02	0.95±0.05	0.99±0.07
C$+A$	1.61±0.02	1.30±0.02	1.00±0.06	

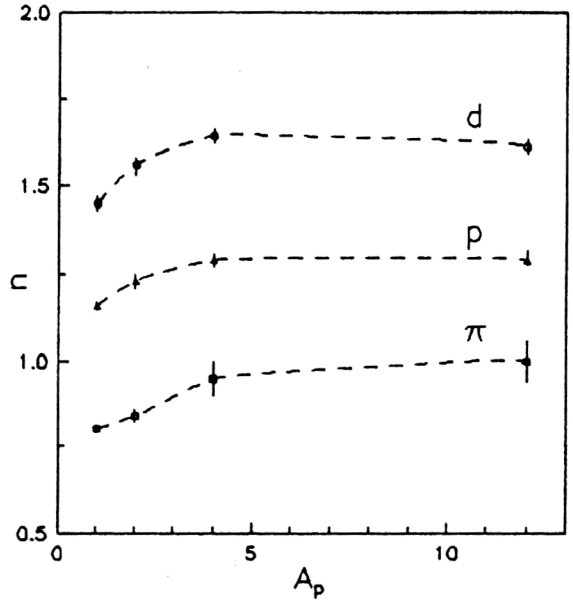

FIG. 11. Values of the exponent n for various beams.

8.9-GeV/c proton beam, and of the energy dependence of the $\pi^\pm$, p, and d cross sections in the momentum range 0.3–0.7 GeV/c. The fragmenting nuclei were ^{58}Ni, ^{64}Ni, ^{64}Zn, ^{114}Sn, ^{124}Sn, and Pb. In Figs. 12–14 we show the data on the A dependence of the cross sections for all the particles of this series of measurements. In Fig. 15 we show the data of Ref. 15 for emission angle 180°. The curve in that figure shows the behavior of the charge density on these nuclei. A jump of the density between the nickel and zinc nuclei is clearly seen, and is manifested uniformly throughout this group of nuclei.

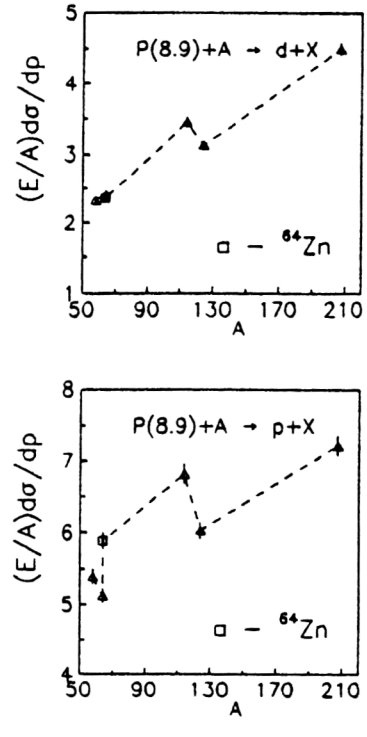

FIG. 12. A dependence of the deuteron and proton cross sections.

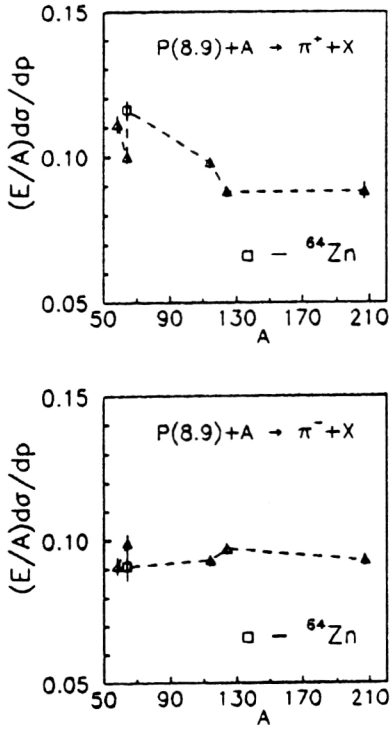

FIG. 13. *A* dependence of the pion cross sections.

We see that the general behavior of the cross sections is similar to that studied in the preceding section and confirms our earlier results[46] about the independence of the cross sections for positively charged particles of the neutron excess.

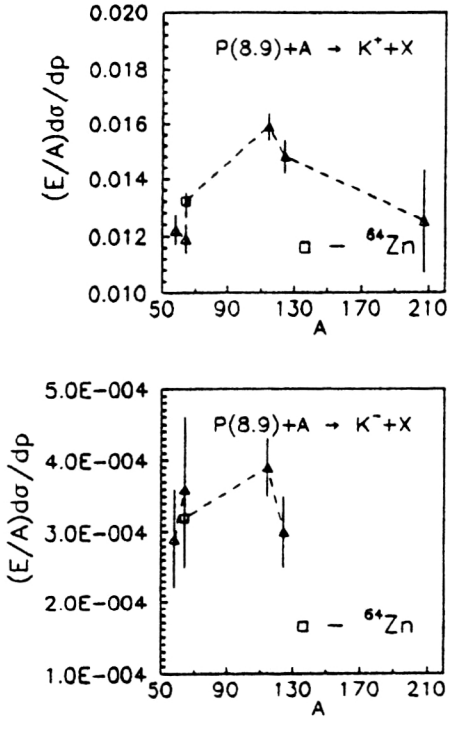

FIG. 14. *A* dependence of the kaon cross sections.

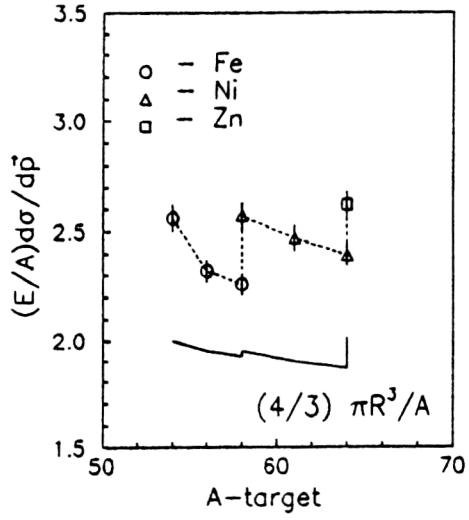

FIG. 15. *A* dependence of the proton cross sections, $p=0.5$ GeV/c, $\vartheta=180°$.

Unfortunately, no definite conclusions can be drawn regarding the K^--meson data-owing to their poor statistical reliability.

The quantitative data are given in Table V in the form of cross-section ratios for various fragmenting nuclei and particles (the cross sections are not normalized to A).

Here we see the same regularities as for proton beams of half the momentum. Positively charged particles follow the proton content, and negatively charged ones follow the neutron content. The cross-section ratios for deuterons occupy an intermediate position.

The energy dependence. The study of cumulative particle production on nuclei with various neutron contents at fixed nuclear charge (separated isotopes) has a rather long history. The goal has been to determine the possible contribution of the most exotic nuclear systems to cumulative processes, because the initial hypothesis about the cumulative effect[1] presupposed that the nuclear form factors have a negligible effect in the hard part of the spectra. The first experimental results[47] confirmed the initial assumption[1] at a level of $\simeq 10-15\%$, and the later results cited above revealed more details.

The present study is the first to investigate the isotopic effect in detail in the momentum range 0.3–0.7 GeV/c. The main results are presented in Refs. 37 and 48. Here we shall use the tabulated data and the results of their approximation from Ref. 41, which are contained in the Appendix.

TABLE V. Cross-section ratios (not normalized to A) on isotopic nuclei ($p=0.5$ GeV/c, $\vartheta=120°$, $P_0=8.9$ GeV/c).

Process	^{64}Ni/^{58}Ni	^{64}Zn/^{64}Ni	^{124}Sn/^{114}Sn
$p+A\to d$	1.03±0.03	0.98±0.03	0.98±0.03
$p+A\to p$	1.05±0.03	1.15±0.03	0.96±0.03
$p+A\to\pi^+$	0.99±0.03	1.16±0.04	0.99±0.03
$p+A\to\pi^-$	1.20±0.04	1.09±0.04	1.13±0.03
$p+A\to K^+$	1.07±0.06	1.11±0.05	1.01±0.05

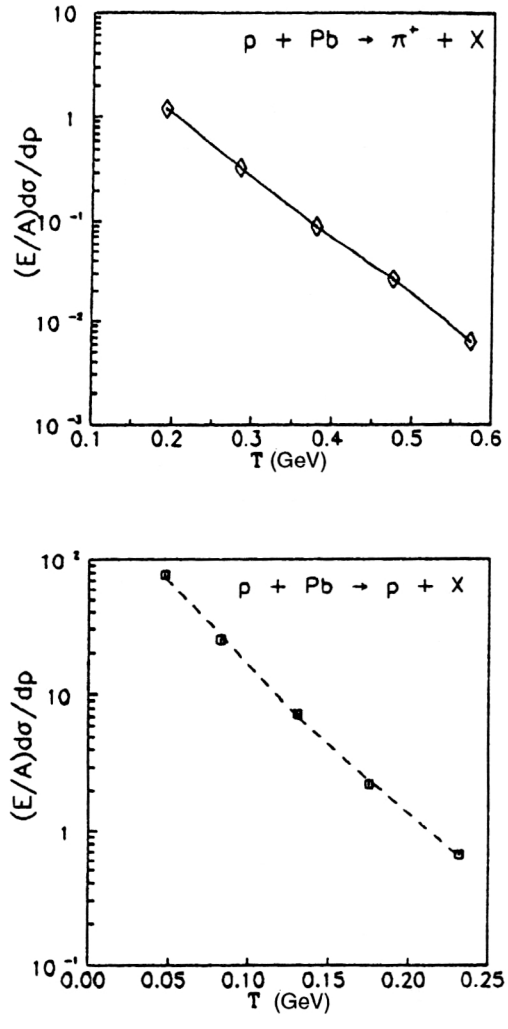

FIG. 16. Energy dependence of the pion and proton cross sections.

The energy dependence of the cross sections for cumulative particle production at emission angle $\vartheta = 120°$ or similar values has been studied by us[14,15] and by others[16–22,45,49] on various nuclei and at various initial energies. For identical kinematical conditions our data agree with the others within the experimental error and the absolute normalization of the cross sections. As mentioned above, the energy spectra behave exponentially in various representations with the corresponding slope parameters. Since the spectra on different nuclei are similar, as an illustration we give the energy spectra of protons and pions on the Pb nucleus, studied together with the isotopic nuclei. These spectra are shown in Fig. 16. The data on the energy dependence were fitted by the exponential expressions[1–3] given above. The parameters of the fit for specific nuclei are given in the corresponding tables of the Appendix. In the measured momentum range for protons and π^- mesons the data are better described by two exponentials, and therefore the measured momentum range was split into two parts, conventionally referred to as the soft (0.3–0.5 GeV/c) and hard (0.5–0.7 GeV/c) regions. The general results of the fit are given in Table VI.

We see from the data of this table that there are clear differences between the slope parameters in the soft and hard

TABLE VI. Weighted mean values of the slope parameters.

	Interval (GeV/c)	T_0 (MeV)	x_0	α_0
p	0.3–0.5	33.4±0.4 $\chi^2=6$	0.097±0.0012 $\chi^2=9$	0.081±0.001 $\chi^2=6$
	0.5–0.7	44.8±0.3 $\chi^2=1.3$	0.114±0.004 $\chi^2=1$	0.092±0.001 $\chi^2=1$
π^-	0.3–0.5	78.9±1.3 $\chi^2=9$	0.161±0.003 $\chi^2=19$	0.129±0.002 $\chi^2=7$
	0.5–0.7	72.5±0.4 $\chi^2=1$	0.153±0.001 $\chi^2=1$	0.117±0.001 $\chi^2=1$
π^+	0.3–0.7	72.6±0.2 $\chi^2=1$	0.150±0.005 $\chi^2=1$	0.118±0.001 $\chi^2=1$
d	0.5–0.7	29.3±0.3 $\chi^2=2$	0.102±0.001 $\chi^2=2$	0.082±0.001 $\chi^2=3$

regions. In addition, the values of χ^2 characterizing the slope parameters in the soft part of the spectra are quite large. This may be associated with the small error, and if so, the exponential dependence does not hold with this accuracy. Another reason might be the fact that the slope parameters for specific nuclei are quite different. In the case of protons, for example, on the ^{124}Sn nucleus, the slope parameter is $\simeq 4\%$ higher than that for the other nuclei. Similarly, for π^- mesons the slope parameter is $\simeq 10\%$ higher for Pb and ^{124}Sn nuclei (see the Appendix). The data of Table VI for deuterons are avaliable only in one momentum range, because the initial momentum was 0.5 GeV/c.

Comparison of the data for 4.5- and 8.9-GeV/c proton beams. It is interesting to compare some characteristics of cumulative production on the same nucleus which are used in measurements in primary proton beams with momentum differing by a factor of two. First we consider the ratio of the π^+- and π^--meson cross sections, presented in Table VII.

The data of this table show that these ratios are nearly the same in the two beams within the experimental error, and they demonstrate another type of detailed scaling in cumulative pion production. A second interesting possibility is the direct comparison of the cross sections in the two beams for all (sufficiently statistically reliable) particles on the same nuclei. These data are given in Table VIII.

Here we see that the proton cross sections for the 8.9-GeV/c beam are very close to those at half the momentum,

TABLE VII. Ratios of the π^+/p^- cross sections for various beams.

A	$P_0=4.5$ GeV/c	$P_0=8.9$ GeV/c
^{58}Ni	1.21±0.03	1.21±0.04
^{64}Ni	0.97±0.03	1.01±0.04
^{64}Zn	1.13±0.04	1.27±0.08
^{114}Sn	1.06±0.03	1.05±0.03
^{124}Sn	0.89±0.03	0.91±0.03
Pb	0.97±0.03	0.95±0.04

TABLE VIII. Ratios of the cross sections for different proton beams (8.9/4.5).

A	d	p	π^+	π^-
^{58}Ni	1.14±0.03	0.86±0.03	1.31±0.03	1.30±0.03
^{64}Ni	1.15±0.03	0.90±0.03	1.32±0.03	1.27±0.04
^{64}Zn	1.13±0.03	0.98±0.03	1.47±0.05	1.30±0.06
^{114}Sn	1.45±0.03	1.07±0.03	1.42±0.05	1.43±0.04
^{124}Sn	1.31±0.03	1.06±0.03	1.42±0.05	1.30±0.04
Pb	1.41±0.03	1.12±0.03	1.54±0.04	1.58±0.05

while the pion cross sections grow and the deuteron cross sections are undecided, showing considerable growth beginning with tin. The individual properties of the nuclei might play a role here. However, a unique A dependence of the cross-section ratio is observed for all the particles: the cross-section ratios grow by about 20% in going from nickel to lead.

DISCUSSION OF THE EXPERIMENTAL RESULTS

Preliminary summary. The results of the preceding sections show that the A dependences of the cross sections in proton and nucleus beams are similar for all the particles observed in this study. Moreover, this similarity persists in the detailed behavior of the cross sections. For light nuclei we see correlations between the cross sections and the nuclear density, which are identical for both pA interactions (primary proton momentum 8.9 GeV/c, emission angle 180°) and DA interactions (momentum per nucleon 4.5 GeV/c, emission angle 120°).

In the region of intermediate and heavy nuclei the detailed similarity is manifested in the behavior of the cross sections on separated isotopes of nickel, zinc, and tin. The scale of variation of the cross sections is comparable to the relative proton and neutron content in these nuclei, and correlations are observed between the production cross sections of positively charged particles and the proton content, independently of the neutron excess, and between the cross sections for negatively charged particles (pions) and the neutron content. These features (the isotopic effect) occur for both proton and nucleus beams. A change of the primary proton momentum by a factor of two does not affect the scale of variation of the secondary-particle cross-section ratios, i.e., the isotopic effect persists in the behavior of the cross sections.

The π^+/π^- cross-section ratios on light and heavy nuclei are identical for proton and nucleus beams.

The p/π^+ cross-section ratios for the same nuclei and beams have a similar behavior, differing only in the value of the ratio on light and heavy nuclei (^{6}Li and Pb, respectively).

The energy behavior of the cross sections on separated isotopes of nickel, zinc, and tin is exponential in all representations, and, except in the case of positive pions, is characterized by two exponentials which distinguish the soft and hard parts of the spectrum. However, according to the χ^2 criterion the exponential representation of the spectra in the soft region is not satisfactory at this level of experimental error, especially for protons.

The exponents of the A dependence of the cross sections for pions, protons, and deuterons behave similarly as a function of the mass number of the projectile and tend to a constant (different for each particle) beginning with beams of He nuclei, i.e., the exponent n depends on the projectile mass in going from a proton to a deuteron beam (we recall that the proton and nucleus beams in this series of experiments had a momentum of 4.5 GeV/c per nucleon).

Direct comparison of the cross sections for 8.9- and 4.5-GeV/c proton beams (in both cases the secondary-particle momentum is 0.5 GeV/c) for identical nuclei and secondary particles reveals a unique A dependence of the cross-section ratios: these ratios grow by about 20% in going from nickel to lead nuclei. The absolute values of the cross sections for protons are close for both primary beams, and the pion cross sections grow with increasing initial momentum.

Ratios of the structure functions. As mentioned in the Introduction, the experimental results on cumulative particle production led to understanding of the quark–parton structure function of the nucleus. The cross section for the inclusive process (4) is described by[28,50]

$$E_1 \frac{d\sigma_{\mathrm{I}}^{\mathrm{II}}}{d\mathbf{p}_1} = C_q^1 \sigma_q^{\mathrm{I}} G_{\mathrm{II}/q}(x, p_{1\perp}^2). \tag{11}$$

Here E_1 and p_1 are the energy and momentum of inclusive particle 1; C_q^1 is a constant characterizing the hadronization of a quark q into hadron 1; σ_q^{I} is the cross section of the process in which a quark q from nucleus II passes through the target I without collisions; $G_{\mathrm{II}/q}(x, p_{1\perp}^2)$ is the quark–parton structure function of nucleus II, interpreted as the quark momentum distribution in the nucleus. It follows from this expression for the inclusive cross section that the ratio of the inclusive cross sections of different fragmenting nuclei II′ and II is equal to the ratio of their structure functions:

$$E_1 \frac{d\sigma_{\mathrm{I}}^{\mathrm{II}'}}{d\mathbf{p}_1} \Big/ E_1 \frac{d\sigma_{\mathrm{I}}^{\mathrm{II}}}{d\mathbf{p}_1} = \frac{G_{\mathrm{II}'/q}(x, p_{1\perp}^2)}{G_{\mathrm{II}/q}(x, p_{1\perp}^2)}. \tag{12}$$

The properties of the nuclear structure functions have been studied in Refs. 14 and 15 for a wide range of fragmenting nuclei and initial energies. A remarkable result in the study of cumulative particle production was the establishment of the relations

$$E_1 \frac{d\sigma}{d\mathbf{p}_1}(\pi^-) \simeq E_1 \frac{d\sigma}{d\mathbf{p}_1}(\pi^+) \simeq E_1 \frac{d\sigma}{d\mathbf{p}_1}(K^+) \gg E_1 \frac{d\sigma}{d\mathbf{p}_1}(K^-). \tag{13}$$

These relations are valid for identical values of the scaling variable x for all particles and confirm the assumptions of Refs. 28 and 50. Since nuclei predominantly contain valence u and d quarks, the equality of the K^+ and π^+ cross sections can be viewed as a consequence of the fact that their structure functions $G_{\mathrm{II}/u}(x, p_\perp^2)$ are identical. In addition, it can be assumed that $C_d^{\pi^-} \simeq C_u^{\pi^+} \simeq C_u^{K^+}$. The K^- cross section is significantly smaller because this meson does not contain valence quarks.

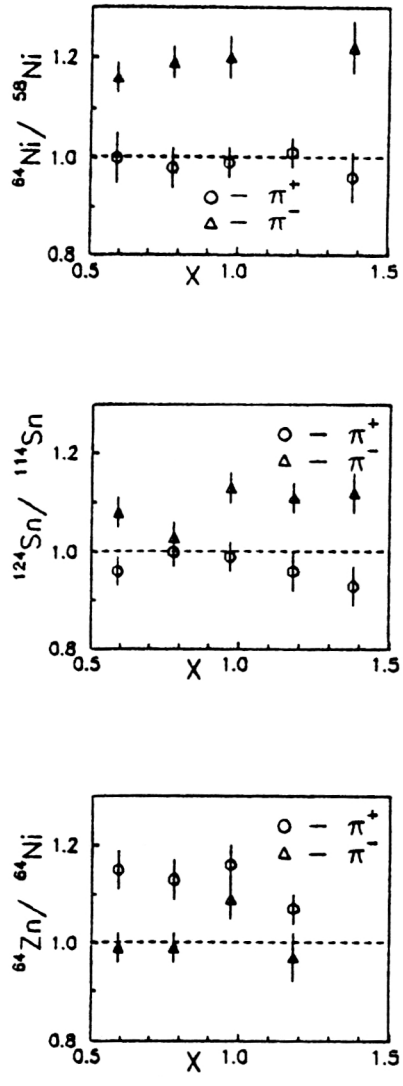

FIG. 17. π^+/π^- cross-section ratio as a function of the scaling variable x.

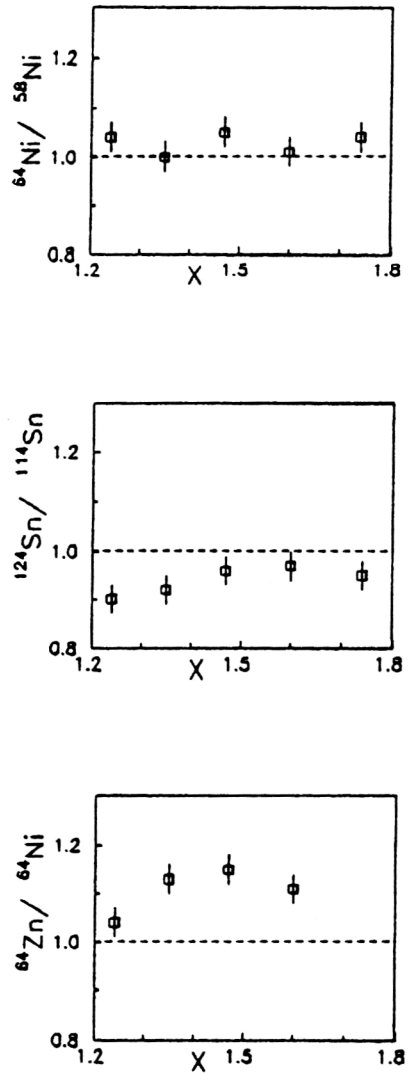

FIG. 18. Ratio of the proton cross sections as a function of the scaling variable x.

The ratios of the structure functions on nuclei of separated isotopes of nickel, zinc, and tin for pions and protons were first studied in Ref. 48 as a function of the scaling variable x; this is equivalent to study of the energy dependence of the isotopic effect for these particles. The results are shown in Fig. 17 (pions) and Fig. 18 (protons).

Let us consider the pion data. The cross-section ratio for the combination $^{64}Ni/^{58}Ni$ is practically unity for π^+ and about 1.2 for π^- in the entire range of x. These nuclei contain identical numbers of protons ($Z=28$) and different numbers of neutrons, $N=36$ and 30, respectively. The ratio of the π^+ and π^- cross sections for the combination $^{124}Sn/^{114}Sn$ behaves similarly. This pair of nuclei also contains the same number of protons ($Z=50$), and the numbers of neutrons are $N=74$ and 64, respectively. The last combination $^{64}Zn/^{64}Ni$ shows that the π^- cross sections are practically equal, and that the π^+ cross section is greater than unity. The proton and neutron contents in these nuclei are 30 and 34 (Zn) and 28 and 36 (Ni). In the last case the numbers of protons and neutrons in the nuclei are different for identical mass numbers (isobars), but the dominant role played by the nuclear charge is apparent.

The same combinations of nuclei for the ratio of the proton cross sections (Fig. 18) show that the proton production cross section is independent of the neutron excess on isotopes of nickel in the entire range of x. The x dependence of the cross-section ratio in the soft region of the spectrum can be traced for tin isotopes. The last combination (zinc and nickel isotopes) demonstrates the effect of the nuclear charge, which is comparable in magnitude to that for pions, and indicates that the soft part of the spectrum depends on x.

The close relation between cumulative processes and deep-inelastic scattering of leptons on nuclei was seen even in the early period of the investigations. In particular, a similar behavior of the structure functions studied in cumulative production and lepton–nucleus scattering was specially noted in Refs. 46 and 50–52. The universal nature of the structure functions in hadron–hadron and lepton–lepton deep-inelastic scattering when the structure of the primary hadron is taken into account was stressed in Ref. 53, where

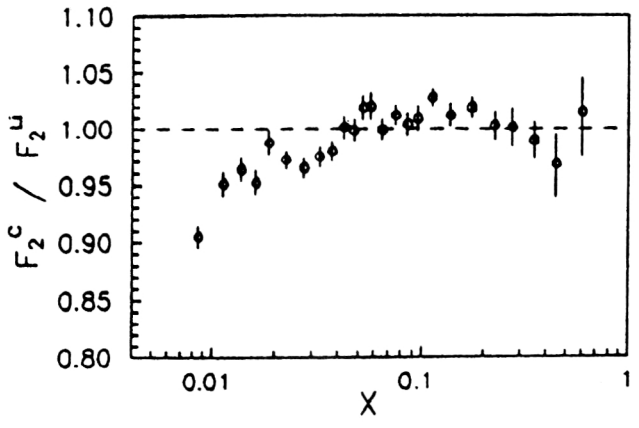

FIG. 19. Ratio of the structure functions of deep-inelastic scattering in the process $\mu(90\ \text{GeV})+A$ from Ref. 56.

the results of investigations of inclusive processes over a long period of time are summarized.

The studies of lepton deep-inelastic scattering on nuclei undertaken in the last decade at various accelerators have revealed interesting features in the behavior of the structure functions, which turned out to be different for free nucleons and nucleons in a nuclear medium. The history of the subject and the results obtained by various collaborations can be found in Ref. 54. The recent data of the BCDMS collaboration[55] are particularly interesting, as they apparently definitively confirm that the structure function F_2^C is nonzero for $x \geqslant 1$ in the scattering of 280-GeV muons on carbon.

The relatively recent data of the New Muon Collaboration[56] (NMC at CERN) on the scattering of 90-GeV muons on ^{6}Li, ^{12}C, and ^{40}Ca nuclei indicate interesting features in the ratios of the structure functions. The selected nuclei differ in their dimensions and densities. They are $r=2.6$ F and $\rho=0.04$ F^{-3} for ^{6}Li, $r=2.5$ F and $\rho=0.09$ F^{-3} for ^{12}C, and $r=3.5$ F and $\rho=0.11$ F^{-3} for ^{40}Ca. The ratios of the structure functions on these nuclei turn out to be sensitive to the nuclear sizes and densities in the range $x \approx 0.008-0.05$. As an illustration, in Fig. 19 we give one of the results of Ref. 56.

COMPARISON WITH THE DATA IN THE LITERATURE

The results presented in the preceding sections reveal the general regularities of cumulative processes: the absolute values of the invariant differential cross sections, the behavior of their A dependence, and the exponential variation of the cross sections in various representations. The correlation between the cross sections and the nuclear density is, in our opinion, the first experimental fact suggesting a reason for the strong variation of the cross sections and their irregular behavior for light nuclei. In any case, this fact determines the sizable value of the cross section for all the particles observed experimentally. The interesting feature in the behavior of the cross sections on ^{4}He and ^{6}Li nuclei (the cross sections per nucleon are identical) may be related to the fact that in an inclusive process we obtain an averaged picture, whereas in some cases the ^{6}Li nucleus acts like the core of the helium nucleus with a deuteron outside the closed shell. Since the ^{7}Li nucleus has much smaller radius than does ^{6}Li (Ref. 57), this region of nuclei is very suitable for performing correlation experiments, which are quite easy to design from the viewpoint of the choice of particle and the momentum and angular detection ranges.

In the region of light nuclei there are interesting features associated with the behavior of the cross sections for cumulative particle production in various beams. The proton and neutron yields from ^{6}Li, ^{7}Li, Be, ^{10}B, ^{11}B, and C were studied in Ref. 58 using proton beams with momentum 7.5 GeV/c and π^- beams with momentum 5 GeV/c at an angle of 120°. The A dependence of the cross sections behaves irregularly for isotopes of lithium and boron. The proton yield increases with increasing number of neutrons, and the charge of the incident particle plays a significant role for isoscalar nuclei: more neutrons are produced in π^-A interactions, while the proton yield is higher in pA interactions. The following values were obtained[14,15] for the cross-section ratio on isotopes of lithium using an 8.9-GeV/c proton beam ($\vartheta=180°$, momentum 0.5 GeV/c): 1.75 ± 0.53 (d), 1.24 ± 0.04 (p), 1.02 ± 0.09 (π^+). The cross-section ratios on lithium isotopes (^{7}Li/^{6}Li) for a beam of carbon nuclei obtained in Ref. 41 are 1.43 ± 0.11 (d), 1.22 ± 0.03 (p), 1.39 ± 0.08 (π^+), and 3.2 ± 2.4 (K^+). Thus, the isotopic effect on light nuclei is manifested in pA interactions only for pions. In CA interactions for all particles the cross sections are observed to grow with increasing number of neutrons in the nucleus (see the tables of cross sections in the Appendix), i.e., the isotopic effect in the sense of the cross sections for positively charged particles being independent of the neutron excess is not observed. Here we see a second feature which is manifested in carbon beams. In connection with this, we note the results of Ref. 59 on the measurement of the spectra of protons, deuterons, and tritium in CA interactions (emission angle 160°). Comparison with the data from pA interactions showed that the slope parameters of the deuterium and tritium spectra are increased for a carbon beam. On the other hand, in Ref. 60 the study of the π^- spectra in pC, DC, αC, and CC interactions did not reveal any change of the shape of the spectra within the 10–15% error. It may turn out that more accurate measurements in nucleus–nucleus collisions will reveal important details of the interaction mechanism. A phenomenological approach to the description of cumulative production in nuclear collisions taking into account the presence of fluctons of the projectile and target has been developed in Ref. 61 and awaits experimental testing.

The characteristic features of cumulative protons, in particular, the A dependence of the cross sections and the slope parameter of the spectra on various nuclei, which have been studied using a beam of bremsstrahlung photons with maximum energy in the range from 2 to 4.5 GeV (Ref. 62) turned out to be the same as for proton beams. The proton kinetic energy was measured in the range 65–280 MeV at angles of 45–150°.

The inclusive proton spectra on the standard set of fragmenting nuclei (Be, Al, Cu, Pb) were measured in Ref. 25 using π^-, K^-, and $\bar{p}$ beams of momentum 40 GeV/c. The range of proton kinetic energies was 0.1–0.3 GeV, and the average detection angle was 157.5°. The general regularities

of cumulative processes appear under these experimental conditions: the exponential behavior of the cross sections, the similar behavior of the cross sections for different beams, the independence of the slope parameter of the spectra from the mass number of the fragmenting nuclei (for $A \geqslant 27$), and the difference in the behavior of the cross sections on light nuclei.

The results obtained using neutrino beams are interesting. The interaction of a wide-band neutrino beam with energy 10–200 GeV with photoemulsion nuclei was studied in Ref. 63 (at Fermilab) to observe the cumulative protons. The data obtained on the slope parameter of the proton spectrum and on the A dependence of the cross sections were compared with the data for hadron and antineutrino beams. Within the experimental error the results are the same for different beams and confirm the general regularities of cumulative processes. In addition to the inclusive data, the authors of Ref. 63 studied the multiplicity correlations in events with cumulative protons. Among the interactions studied, those authors saw events without cumulative particles and events with one or more cumulative particles (some even with more than three). It turned out that the average number of relativistic (s) particles is independent of the number of cumulative protons and of whether or not any are present at all. The average multiplicities of b and g particles (protons with momenta 250–1000 MeV/c) are proportional to the number of cumulative protons. The data were analyzed by the authors of that study using the few-nucleon correlation model and the mean-field model, and it was found that there are no correlations between $\langle x_a \rangle$, the average value of x for events with cumulative protons, and $\langle x \rangle$, the average value of x for the other events. This result disagrees with the predictions of those models.

The same neutrino beam was used in Ref. 64 to study the depenence of the average yield of cumulative protons on the squared 4-momentum transfer Q^2 for events with and without cumulative protons. It was found that in the range of neutrino energies 10 GeV$\leqslant E_\nu \leqslant$30 GeV, the value of $\langle Q^2 \rangle$ is independent of the presence of cumulative protons in the events. In the range 30–50 GeV the value of $\langle Q^2 \rangle$ is larger for events with cumulative protons than for ones without them. For $E_\nu > 50$ GeV the value of $\langle Q^2 \rangle$ is smaller in events with cumulative protons than in ones without them. For $E_\nu > 50$ GeV and $Q^2 > 15$ (GeV/c)^2 the average yield of cumulative protons falls sharply (by about a factor of 4). This led the authors of Ref. 64 to conclude that as E_ν and Q^2 increase, the momentum transferred to the parton jet increases, and, in accordance with the hypothesis of finite hadron formation length, the contribution of secondary interactions decreases. At sufficiently large momentum transfers hadrons can be formed outside the nucleus, which causes the contribution of secondary interactions to die out.

Similarity of the characteristics of cumulative protons and neutrons was noticed in Ref. 65, where the proton and neutron yields were studied for a large group of nuclei using proton beams of momentum 7.5 GeV/c and $\pi^\pm$ beams of momentum 1.4 and 5 GeV/c. The secondary-particle kinetic energies were measured in the range 60–200 MeV at the angle 120°. The proton and neutron spectra on different nuclei and beams are similar. The ratios of the neutron and proton cross sections are close for heavy nuclei on different beams, and they demonstrate scaling behavior as a function of the secondary-particle energy. It is remarkable that these ratios are smaller than N/Z, the relative content of neutrons and protons in the nuclei studied.

The spectra of cumulative particles (protons and pions) were measured in Ref. 19, for kinematical conditions close to those of the present study, in the secondary-particle momentum ranges 0.6–1.8 GeV/c (protons) and 0.6–1.6 GeV/c (pions) for emission angle 119°. This is the largest momentum range for an initial energy of 10 GeV. Our data were compared with the results of Ref. 19 (cross sections per nucleon of the fragmenting nucleus) for Pb and Ta nuclei with similar A values, taking into account the absolute normalization of the data. The fit to the proton data[19] gives the average value $\langle x_0 \rangle = 0.134 \pm 0.002$ in the entire range of x. The fit to the combined data reveals two exponentials with slope parameters 0.136 ± 0.002 and 0.08 ± 0.006. Similarly, for the combined pion data we find $\langle x_0 \rangle = 0.145 \pm 0.002$ (π^+) and $\langle x_0 \rangle = 0.150 \pm 0.002$ (π^-), but in the latter case the value of χ^2 is over 30. The original values of the slope parameters in Ref. 19 for pions were 0.140 ± 0.002 (π^+) and 0.137 ± 0.002 (π^-). The slope parameters of our data for pions of different sign agree for momenta above 0.5 GeV/c and exceed the values in Ref. 19 by about 10%. On the other hand, the slope parameter of the proton spectrum is about 15% smaller than that in Ref. 19. This discrepancy arises because in Ref. 41 we obtained the slope parameters by separate fitting of the regions arbitrarily designated as the soft and hard parts of the spectrum, which is not really correct for a small number of points. Our goal there was to obtain the most acccurate value of the slope parameters for individual nuclei (see the corresponding tables of the Appendix).

The ratios of the π^+ and π^- cross sections in Ref. 19 are identical and within the experimental error (10%) independent of the mass number of the fragmenting nucleus. These ratios increase from 1.1 to 1.3 in the pion momentum range 0.6–1.4 GeV/c. Possible reasons for the pion cross-section ratios to differ from unity are the following: the effect of the incident-particle charge or of the Coulomb field of the nucleus, the neutron excess in the nuclei, or the difference between the structure functions of u and d quarks in isotopically asymmetric nuclei. All of these factors can apparently affect the cross-section ratio, but so far a satisfactory explanation is lacking.

According to the data of Ref. 24, which summarizes a large series of studies by those authors, the dependence of the π^-/π^+ cross-section ratios on the pion momentum shows that the ratios deviate from unity by less than 20%, and a significant momentum dependence can be seen only for the tungsten nucleus.

A number of interesting results were obtained in Ref. 66 from study of the process $p + A \to \pi^\pm(180°) + X$ on the C, Al, Cu, Sn, and Pb nuclei. The measurements were performed in proton beams of energies 0.8, 1.05, 2.1, 3.5, and 4.89 GeV. First, the π^-/π^+ cross-section ratio grows with increasing initial energy and reaches unity for initial energy $\sim$5 GeV. The slope parameter of the pion spectrum T_0 be-

haves similarly as a function of the energy of the proton beam, reaching a constant value of ~60 MeV for initial energy of the proton beam ~5 GeV.

The behavior of the exponent of the A dependence of the pion cross sections has special features at different initial proton energies. For the energies 0.8 and 1.05 GeV it is constant, equal to about 2/3. Then it rises to unity at the value of the scaling variable used in Ref. 66, $K=T_\pi/T_\pi^{\max}\geqslant 1$ (the cumulative region), where $T_\pi^{\max}$ is the maximum possible kinetic energy of pion production in a nucleon collision. The pion energy spectra have an exponential form in the dependence of the cross sections on the scaling variable $x'=p_\pi^{\text{c.m.}}/(p_\pi^{\text{c.m.}})_{\max}$. The slope parameters of the spectra are different for each initial proton energy. The scaling behavior of the cross sections for negative pions as a function of the variable $(1-x')^N$ following from the hard-scattering model is not confirmed by the experimental data. The results of Ref. 66 confirm the main features of cumulative production and, in addition, demonstrate the attainment of the asymptotic regime for initial energy equal to 4–5 GeV, in agreement with Refs. 13 and 7.

Let us consider the π^+/π^- cross-section ratio from the viewpoint of the isotopic invariance of the strong interactions.[1] Denoting the invariant differential cross section as $Ed\sigma/d\mathbf{p}=f$, for the elementary event we can write

$$f(p\to\pi^+nX)=f(n\to\pi^-pX)=f_N,$$

$$f(p\to\pi^-\Delta^{++})=f(n\to\pi^+\Delta^-)=f_\Delta,$$

$$f(p\to\pi^+\Delta^0)=\frac{1}{3}f_\Delta,$$

$$\frac{f_\Delta}{f_N}=\xi\ll 1 \quad (\xi\simeq 0.1-0.01).$$

In the case of the ^{58}Ni and ^{64}Ni nuclei with numbers of protons and neutrons Z,N and $Z,N+\Delta N$, respectively, we have $y\equiv\Delta N/N=0.2$. Similarly, for the pair of nuclei ^{64}Ni and ^{64}Zn we have $y'\equiv\Delta Z/Z\simeq 0.07$. Then for the ratio of cross sections on nuclei with different numbers of protons and neutrons Z_1,N_1 and Z_2,N_2 we obtain

$$R(\pi^+)\simeq\frac{Z_1f_N+N_1f_\Delta}{Z_2f_N+N_2f_\Delta}\simeq\frac{Z_1}{Z_2},$$

$$R(\pi^-)\simeq\frac{Z_1f_\Delta+N_1f_N}{Z_2f_\Delta+N_2f_N}\simeq\frac{N_1}{N_2}.$$

Finally, for the ratio of cross sections on nuclei which are isotopes and isotones we obtain

$$R(\pi^+)\simeq 1;\quad R(\pi^-)\simeq 1+\frac{\Delta N}{N}\simeq 1+y \quad \text{(isotopes)}, \tag{14}$$

$$R(\pi^+)\simeq 1+\frac{\Delta Z}{Z}\simeq 1+y';\quad R(\pi^-)\simeq 1 \quad \text{(isotones)}. \tag{15}$$

We see from the latter expressions that the ratios of the π^+ and π^- cross sections are determined only by the relative content of protons and neutrons in the nuclei and do not involve any additional factors which could take into account other characteristics. The general values for the cross-section ratios are in quite satisfactory agreement with the experimental values quoted above for proton and nucleus beams of various initial energies and emission angles (Tables III, V, and VII). This viewpoint preserves the succession with the elementary event and reflects the general conservation laws. However, the results on light and heavy nuclei are not described in this scenario. We recall that on light nuclei the cross sections are observed to grow with increasing number of neutrons, while on heavy nuclei the cross sections for positive and negative pions are about the same.

In Ref. 37 the irregularities in the behavior of the cross sections for positive particles on isotopically enriched nuclei were associated with the change of the nuclear charge radii, the known values of which were used to calculate the density per nucleon of the nucleus (the charge-distribution density). It was noted that the cross sections are correlated with the charge-distribution density determined in this manner. Figure 15 shows the data on the proton production cross section and the values of $4\pi R^3/3A$ for isotopes of iron, nickel, and zinc (here R stands for $\langle r^2\rangle^{1/2}$). The slight hint of a jump in the curve in going from ^{58}Fe to ^{58}Ni is related to the fact that there are several values of the rms radii for these isotopes, calculated using different models.[40] We chose the average radius, which could level out the result. The existence of this correlation, which has the same magnitude for particles with different kinematical and quantum characteristics, is very interesting for understanding the interaction of relativistic nuclei. We stress the following: the collision parameter was not controlled in the experiment.

We see that the main characteristics of cumulative particle production are quite insensitive to the form and energy of the primary particle beams. The data of the present study demonstrate this stability for nuclear targets, in detail in some cases. Before summarizing the results, let us study the most popular models of cumulative production. We make no claim that our discussion is complete and do not go into the details of the original studies. We note only the main features which can be directly compared with the experimental results.

POSSIBLE MECHANISMS OF CUMULATIVE PARTICLE PRODUCTION

Unavoidable accompaniments of processes involving nuclei are the Fermi motion of the nucleons and the rescattering of the created particles on intranuclear nucleons if they are created inside the nucleus. Naturally, the question of the contribution of the Fermi motion arose in connection with the first discovery of cumulative pions[2] in the process D $+\text{Cu}\to\pi^-(0°)$. The calculations performed in Ref. 67 showed that the experimentally observed cross sections are about two orders of magnitude larger than the possible contribution from the Fermi motion. Direct calculation of the experimental spectrum of pions from nuclei[68] showed that in the hard part of the spectrum the effect from the contribution of the Fermi motion is smaller than the observed effect by

4–5 orders of magnitude. Here it is appropriate to note that the work done in Ref. 69 essentially reproduced the experiment of Ref. 2. The fragmentation of the incident deuteron into π^- on C, Al, Cu, and Pb targets was studied in order to explain the dependence of the cross section for projectile fragmentation on the type of target. The exponents n proved to be 0.27 ± 0.09, which indicates that the interaction has a peripheral nature. A similar conclusion was made in Ref. 70 in studying the fragmentation of a beam of helium nuclei into π^- (the exponent $\alpha=0.4$).

The contribution of successive rescatterings on intranuclear nucleons was calculated in Ref. 71 for cumulative proton production, and qualitative agreement with experiment was obtained. The characteristic features of the multiple-scattering mechanism are the presence of recoil nucleons and polarization of the final protons, which must accumulate in successive scattering events. The latter feature was not confirmed experimentally. Measurements of the proton polarization on various nuclei using a 1-GeV proton beam gave a zero result on the average.[72] The polarization of cumulative protons in pA interactions for initial proton energies in the range 16–64 GeV is insignificant ($\simeq 10\%$).[73] The role of the production of large masses in the intermediate state in inelastic rescattering on the nucleons of the deuteron, leading to cumulative pion production in the entire kinematically accessible region, was estimated in Ref. 74. The authors showed that the experimentally observed value from Ref. 12 can be obtained in this approach. The studies that we have quoted[71,74] date from the early stage of investigation of cumulative processes, and it is not at all obvious whether or not the logic of these studies incorporates the properties of scaling, detailed scaling, or superscaling which characterize the modern experimental results on cumulative production.

The authors of Ref. 75 were the first to propose a mechanism for cumulative hadron production analogous to the production of hadrons with large transverse momenta on nuclei.[76] The nucleus is treated as a heavy elementary particle consisting of n_A quarks. The incident particle decays into parton–quarks, one of which (or a more complicated quark formation) collides with a parton (or quark formation) of the nucleus and produces a parton with large momentum transfer, which is emitted into the backward hemisphere and is hadronized into a detected particle. For the incident particle, the quarks contained in the volume of radius $r_0 \simeq m_\rho^{-1}$ turn out to be coherent. In the rest frame of the nucleus this volume is dilated by the γ factor, and for sufficiently large initial energy E, when $\gamma > R/r_0$, it cuts a tube from the nucleus. The probability for a single quark to be incident on the coherence volume is equal to the ratio of the cross-sectional areas of the tube and the nucleus: $q \sim (r_0/R)^2 \ll 1$, and the probability for all $3A$ quarks to reach this volume is $(q^2)^{3A}$ and falls off factorially with increasing A. The process on coherent fluctons with smaller quark content is more probable. The cross section for cumulative hadron production in the process $B+A \to C+X$ has the form

$$\varepsilon \frac{d^3\sigma}{d^3p} \simeq \left(\frac{E}{\varepsilon}\right)^{\alpha(0)-1} \cdot A^{2/3} \cdot \frac{\varphi(\varepsilon_\vartheta)}{\varepsilon^{k+1}} \times \exp\left[-\varepsilon_\vartheta B\left(\ln \frac{\varepsilon_\vartheta}{A^{1/3}} \cdot C\right)\right]. \tag{16}$$

Here E, ε, and ϑ denote the energy of the incident particle, the energy of the observed hadron, and the emission angle, $\alpha(0)$ is the intercept of the leading Regge trajectory in the $B\bar{B}$ channel, $\varphi(\varepsilon_\vartheta)$ is a power-law function of ε_ϑ, C is a constant parameter, and $k=n_a+n_b+n_c-2$, where n_i is the quark content of the interacting flucton formations of the incident particle and the observed hadron. The function $B(L)$ is monotonic in the region $L>0$, $B(0)=0$, and $B \sim L$ for $L \to \infty$. The specific form of this function depends on the clustering in the nucleus, i.e., on how large are the groups of quarks in the coherent fluctons. This expression describes the characteristic features of cumulative processes: for $\alpha(0)=1$ the cross section is independent of the initial energy, and with increasing A the cross section grows roughly as A^n, where $n=\frac{2}{3}+\varepsilon_\vartheta^{1/3}\langle B/L\rangle$. The slope B grows with increasing mass of the incident particle (ε_ϑ) and decreasing A, and the cross section is isotropic for small momenta ($p/\varepsilon \ll 1$) and falls for $p \simeq \varepsilon$. The quantitative description depends on the model of flucton formation.

The quark–parton model of production on nuclei at high energies was developed in Ref. 77 and gives a good reproduction of the experimental results on the deep-inelastic scattering of leptons on nuclei, on lepton-pair production, on cumulative pion production, and for processes with large values of x and small $p_\perp$. The model is based on the concept of the fragmentation of a group of nucleons lying inside a tube of cross section σ oriented along the trajectory of the incident particle. The nucleons inside the tube are assumed to be inactive at the time of the collision and are spectators whose interaction is neglected. The inelastic cross section on the nucleus has the form

$$\sigma_A(a \to b) = \frac{\sigma_A}{\sigma} \cdot \sum_{i=1}^{A} P(i,A)\sigma_i(a \to b), \tag{17}$$

where σ_A/σ is the effective number of nucleons in the tube, $P(i,A)$ is the probability that the tube contains exactly i nucleons, and $\sigma_i(a \to b)$ is the fragmentation cross section of this tube. The nucleons contained in the tube can be replaced by quarks, assuming that $d_n=u_p$ and $u_n=d_p$ for the $(Z/A)_i$ protons and the $[(A-Z)/A]_i$ neutrons contained in the tube. Then in the frame of the overall momentum of the nucleus the valence quarks of the nucleons in the tube have the following x distributions:

$$u_i(x) = (Z/A)\tilde{u}_i(x) + [(A-Z)/A]\tilde{d}_i(x), \tag{18}$$

$$d_i(x) = (Z/A)\tilde{d}_i(x) + [(A-Z)/A]\tilde{u}_i(x). \tag{19}$$

The forms of the functions d_i, $\tilde{d}_i$, u_i, and $\bar{u}_i$ used in the actual calculations and of the functions describing the recombination of quarks into hadrons are given in Ref. 77.

In Ref. 11 the fragmentation model[77] was used to estimate the isotopic effect for protons and π^+ mesons, which occurs owing to the smallness of the ratio $\tilde{d}_i/\tilde{u}_i \simeq 0.1$. In

addition, the isotopic effect was predicted for K^+ mesons, and the isotonic effect was predicted for π^- mesons and neutrons. These predictions were actually confirmed experimentally, at least qualitatively, and here it would be interesting to have more accurate calculations. As was shown in Ref. 11, the fragmentation model gives a completely successful reproduction of the experimental results for particles consisting of valence quarks. However, calculations give a factor $\simeq 600$ for the K^+/K^- cross-section ratio, which is an order of magnitude larger than the experimental data. The results of the present study for the K^+/K^- ratio give $40\pm 20\%$, $x\simeq 1.2$ in the range of nuclei from Ni to Sn. In the hard-scattering model[11] the K^+/K^- ratio is $\simeq 80$ for the tantalum nucleus (initial energy 400 GeV, $x\simeq 1$). The hard-scattering model leads to too rapid falloff of the cross section for the cumulative process with increasing x, and it is doubtful that a description in terms of a quark–quark scattering mechanism of heavy-fragment (p,d,t) production would work, because even in processes with large p_T the behavior of the proton cross section $(\sim p_T^{-12})$ differs strongly from that of the meson one $(\sim p_T^{-8})$.

The original idea of fluctuations of the nuclear-matter density[6] was developed in Ref. 9 to the current level of understanding. Density fluctuations occur in a small correlation volume $V_\xi \simeq (4/3)\pi r_\xi^3$, where r_ξ is the correlation radius. The initial proton can interact with the correlation as with a single object of mass $M_k = km$, i.e., the flucton mass. The probability for such an event according to the classical theory of an ideal gas (normalized to the A nucleons of the nucleus) is estimated as

$$\beta_k^A = \binom{A}{k}(V_\xi/V_0)^{k-1}A^{1-k} \simeq A \gg k(A/k!)(V_\xi/V_0)^{k-1} \tag{20}$$

for $A \gg k$. Here AV_0 is the nuclear volume and $V_0 = (4/3)\pi r_0^3$ is the nucleon volume for effective radius $r_0 = 1.2$ F. Such a fluctuation has a lifetime τ_k small compared to the period of motion t^A of the orbiting nucleon. The probability is $\beta_k^A \simeq \tau_k / t^A$. The reaction cross section and form factors for scattering on the nucleus A are defined as

$$\sigma = \sum k\beta_k^A \sigma_k; \quad F = \sum k\beta_k^A F_k, \tag{21}$$

where σ_k and F_k are the cross sections and form factors for the interaction of the incident particle with the flucton (k is the number of nucleons in the flucton). They are calculated either phenomenologically by analyzing independent experiments, or microscopically, using quark–parton representations of the hadron– or lepton–flucton interaction mechanism.

Starting from the assumption that the nucleons of the nucleus lose their individuality in the correlation region $r < r_\xi$, the probability β_k^A is redefined as

$$\beta_k^A = b_k^A D_k, \tag{22}$$

where b_k^A is the probability of finding an ordinary (not compressed) cluster of k nucleons in the nucleus A, and D_k is the probability of finding this cluster in a state of fluctuation compression, i.e., it is essentially the probability for a phase transition of k nucleons into a state of a $3k$-quark object. The quantity b_k^A is calculated by the usual methods of nuclear physics. The probability D_k is calculated using one of the models of quantum chromodynamics. Calculation of the probabilities for multibaryon configurations shows that D_k decreases strongly with increasing k and, for example, for $k=4$ is $\sim 10^{-4}$. The probability for a two-baryon system in the deuteron is 8–9% according to the data on deep-inelastic scattering.

The cross sections for cumulative pion and proton production calculated on the basis of flucton representations reproduce the experimental results for $p_\perp = 0$. It is sufficient to introduce fluctons with $k=4$, and in the vicinity of the kinematical limit for the kth flucton the cross section receives a contribution from the following $(k+1)$th flucton at intermediate values of its variable. In all the cases studied (different k and A), the correlation radius r_ξ in the flucton lies in the range from 0.5 to 0.7 F, i.e., it is comparable to the radius of the core of the NN force. The cross sections for $pA \to p$ and $pA \to \pi$ have identical structure. The ratio of the proton and pion cross sections in a particular case ($P_0 = 8.9$ GeV/c, $\vartheta = 180°$, secondary-particle momentum 0.5 GeV/c, Pb nucleus) is 30–150, which agrees qualitatively with experiment. In contrast to reactions with backward particle production, in processes with large transverse momenta the reaction mechanism undergoes a change, when the partons making up the nucleon and the flucton undergo hard collisions with large momentum transfer.

The model of few-nucleon correlations was developed in Refs. 78–81 and was applied to various processes at high energies. This model is based on the hypothesis of a nuclear core, the existence of which leads to a noticeable contribution from configurations in which n nucleons are found at small relative separations. The probability of such a configuration for the deuteron is estimated to be $(4-8)\times 10^{-2}$ and grows with increasing atomic weight of the nucleus. After systematically studying the space-time picture of the scattering process $\gamma + D \to p + X$, the authors came to consider hadron–nucleus processes with the following assumptions.

It is assumed that in passing through the nucleus, a sufficiently fast hadron h knocks out slow nucleons lying at the same impact parameter relative to the incident hadron. The number of such nucleons is $\sim A^{1/3}$. If along its path the fast hadron h encounters a correlated pair, the number of which is $\sim A^{1/3}$, the incident hadron splits this pair and the spectator nucleon is emitted backward with large momentum. As a result, the inclusive spectrum of cumulative nucleons is proportional to $A^{1/3}\sigma_{\text{tot}}hA \sim A\sigma_{\text{tot}}hA$ for a sufficiently heavy nucleus, where nuclear surface effects are unimportant. The splitting of the correlated pair is described, as for the deuteron, by taking into account screening. It is assumed that the hadron h interacts identically with the proton and the neutron, which are distributed uniformly at the center of the nucleus, i.e., the correlation functions ρ_A^{pp} and ρ_A^{pn} are equal. In the geometrical picture, the cross section for the interaction of a hadron h with the nucleus is $\sigma_{\text{tot}}hA = A\sigma hN/N_{\text{eff}}$, where N_{eff} is the average number of nucleons in a tube of cross-sectional area $\pi\rho_h^2$, assuming that the transverse size of the hadron ρ_h is smaller than the characteristic spacing

between the nucleons in the nucleus. A clear realization of this scenario is the Glauber picture, in which the incident hadron interacts with each of the N_{eff} nucleons of the tube independently. The probability of finding in the nucleus a nucleon correlated with any of the N_{eff} nucleons of the tube is

$$\frac{1}{A}\,\rho_A^{NN}(M_{NN}^2)/(2-\alpha), \tag{23}$$

and the cross section for the inclusive process is

$$E\,\frac{d^3\sigma}{d^3p}=\sigma_{\text{tot}}hAN_{\text{eff}}\,\frac{1}{A}\,\frac{\rho_A^{NN}(M_{NN}^2)}{2-\alpha}\,\kappa_h=\sigma_{\text{tot}}\,\frac{\kappa_h\rho_A^{NN}(M_{NN}^2)}{2-\alpha}. \tag{24}$$

Here $\alpha=(\sqrt{m^2+p^2}-p_3)/m$ is the scaling variable. In the replacement of $\sigma_{\text{tot}}hN$ by $\sigma_{in}hN$, κ_h takes into account possible screening in the interaction with the pair and the small suppression due to the final-state interaction. This expression for the cross section is also valid for a heavy nucleus, when there is a noticeable probability for the knockout of several pairs. The condition for it to be applicable is $E_h/N_{\text{eff}}>E_0$, where E_0 is the energy beginning at which the cross section for knockout of a nucleon of momentum p_N from the deuteron depends weakly on the incident-particle energy. For a real nucleus there is a relatively broad distribution in the number of collisions, and the onset of scaling is delayed. This equation is also applicable to the production of cumulative π, K, and Λ.

In the case of formation of fragments $(d,t,\ldots)$ it is assumed that on the average the incident hadron breaks up several correlated pairs of nucleons at the same impact parameter relative to it. The cumulative nucleons from these pairs are combined into the observed fragments in the mean field of the nucleus. This mechanism leads to a relation between the cross sections for fragment production, which are expressed in terms of the cross section for proton creation. For example, for deuteron production we have

$$E_{\text{D}}\,\frac{d^3\sigma}{d^3p_{\text{D}}}=\frac{\xi_{\text{D}}}{p_{\text{D}}^2}\left[\frac{E_p\,\dfrac{d^3\sigma}{d^3p_p}\,(p_{\text{D}}/2)}{A\sigma_{in}^{hN}}\right]^2 A\sigma_{in}^{hN}. \tag{25}$$

This relation is valid for $\vartheta=180°$. The factor ξ_{D} is of order 10^{-2}. A similar expression can be written down for tritium fragments.

In nuclear collisions[44] the universal quantity is (in both γA and hA interactions)

$$f_B^{A/N}(\alpha,k_\perp)=G_B^{A/N}(\alpha,k_\perp)/\sigma_{\text{inel}BN}\kappa_B. \tag{26}$$

Here κ_B is the screening factor in the interaction of an NN pair of nucleus A with nucleus B, and

$$G_B^{A/N}(\alpha,k_\perp)\equiv\alpha\,\frac{d\sigma^{B+A\to N+X}}{d\alpha d^2k_\perp}\,\kappa_B. \tag{27}$$

The quantity κ_B depends only on the mass number of the nucleus B, and not on A. The inclusive cross section for nucleon knockout from a pair (triplet) is practically independent of the interaction of nucleus B with nucleons not belonging to correlations. The B dependence of κ_B is qualitatively determined by the condition that the interaction of nucleus B with the pair (but not with nucleus A) be peripheral, i.e., a few-nucleon correlation must interact only with the edge of nucleus B. Otherwise, spectators are not formed, because they lose their energy in interacting with the nucleons of nucleus B. Since the thickness of the surface layer depends weakly on the mass number of nucleus B, at large B we have $G_B^{A/N}(p_N)\sim B^{1/3}$.

A specific expression of the universality of cumulative particle production in nuclear collisions is the scaling law:[44]

$$G_B^{A_1/p}(p_N)/G_B^{A_2/p}(p_N)=\varphi(A_1,A_2), \tag{28}$$

i.e., the ratio of the inclusive spectra is independent of the type of incident particle (we note that in the original hypothesis of the cumulative effect it is assumed that the characteristics of cumulative processes are independent of the type of colliding objects). Using the expression for the scaling law, we can form the following cross-section ratios:

$$R_1=\frac{\text{He}+A\to p+X}{\text{D}+A\to p+X},\qquad R_2=\frac{\text{He}+A\to p+X}{\text{He}+\text{C}\to p+X}. \tag{29}$$

Here He and D denote the primary beams, and A and C are the fragmenting nuclei. These ratios are shown in Fig. 20. We see from these figures that the ratios R_1 for protons, deuterons, and pions are practically independent of the mass number of the fragmenting nuclei (excluding the region of light nuclei in the case of pions). The ratios R_2 are constant for pions, and for protons and deuterons they are growing functions of A which differ because of their different A dependences. These results are in reasonable agreement with the assumptions of Ref. 44.

The inclusive cross sections in nucleus–nucleus collisions at high energies were studied in Ref. 82 using the Glauber multiple-scattering theory taking into account multinucleon collisions. The AA interaction process is represented as a set of a series of interactions of one or several nucleons of the projectile simultaneously with one or several nucleons of the target. In the nonrelativistic case this set can be represented as successive interactions. At superhigh energies parallel interactions are more likely, where one or several nucleons of the projectile decay into virtual constituents (partons) long before the interaction. These then interact with one or several nucleons or partons of the target, forming observable final particles. The inclusive cross section $I^{(1)}$ for AA collisions is expressed in terms of the inclusive cross sections $\sigma_{ik}^{(1)}$ for simultaneous collisions of i nucleons of the projectile with k nucleons of the target:

$$I^{(1)}=\sum_{i=1}^{A}\sum_{k=1}^{A'}I_{ik}^{(1)};\quad I_{ik}^{(1)}/AA'=\sigma_{ik}^{(1)}w_iw_k'(2m)^{2(i+k-2)}, \tag{30}$$

where w_i is interpreted as the probability of finding i nucleons of the projectile at the same point:

$$Aw_i=i!\,C_A^i(2m)^{3(1-i)}\int d^3x\rho^i(x). \tag{31}$$

A similar expression can be written down for the target (w'). Equation (30) distinguishes the dynamics of the pro-

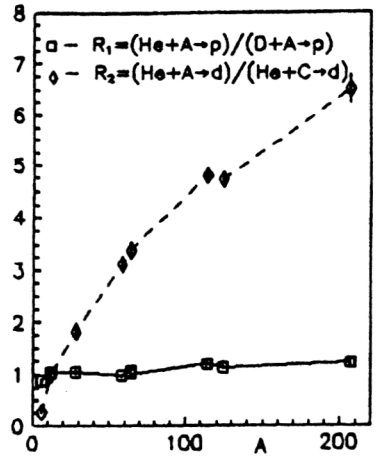

FIG. 20. Ratios of the cross sections for various particles according to the scaling law.

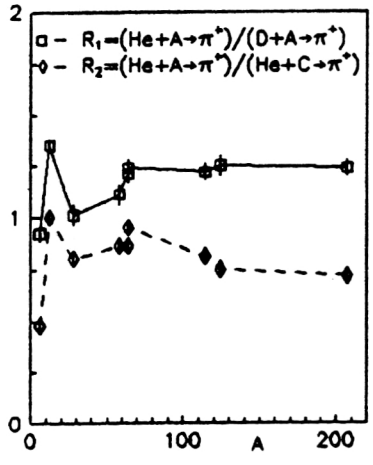

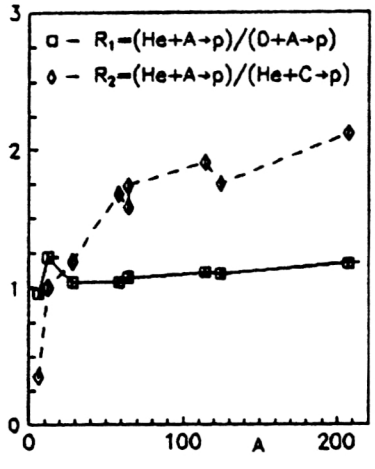

cess at small distances by means of $\sigma_{ik}^{(1)}$ and the geometrical picture of its evolution related to the nuclear structure, which reflect the probabilities w_i and determine the A dependence of the cross sections. The region of the spectra of the cross sections $\sigma_{ik}^{(1)}$ for different i and k differs purely kinematically. The region where $\sigma_{ik}^{(1)} \neq 0$ and $\sigma_{i1}^{(1)} = 0$ is referred to as the cumulative region. If we take $i=1$ and k to be the minimum value allowed in the given kinematics (the approximation of few-nucleon correlations), then in the cumulative region of target fragmentation

$$I^{(1)} \simeq I_{1k}^{(1)} = AA' \sigma_{ik}^{(1)} w_k' (2m)^{2(k-1)}, \tag{32}$$

which is A times larger than the inclusive cross section for cumulative particle production on the nucleus A' by a single nucleon. Experimentally (see Figs. 2–5 and the tables of cross sections in the Appendix), the cross sections for CA interactions exceed those for pA interactions by about a factor of 4.5.

The microscopic picture of the production of light fragments in hadron–nucleus interactions was studied in Ref. 83 in the central region and in the target-fragmentation region. The inclusive process $h+A \to F+X$ was studied, where F denotes the fragment mass number ($F=2-4$). When the momentum of the produced fragment $p_F = Fk$ is directed into the forward hemisphere (the noncumulative region), each parton interacts with only one nucleon of the target nucleus ($n=1$). Owing to the kinematical constraints, in the cumulative region it is impossible to produce a fragment nucleon with the needed momentum k per nucleon, so that the interaction of each incident parton with at least two nucleons of the target nucleus is taken into account ($n \geq 2$). In a collision of a parton with n nucleons of the target nucleus it is possible to produce a fragment nucleon with momentum k belonging to the kinematical region with limits given by $k_-/m = n$, where m is the nucleon mass, $k_- = k_0 - k_z$, $k_0 = (k^2+m^2)^{1/2}$, and $k_z = k \cos \vartheta$. This expression is valid for ultrarelativistic energies of the incident hadron. For $n=2$ in the case of production of a fragment directly backward it follows that the fragment momentum is bounded by the value $3/4m$ per nucleon.

Expressions have been obtained for the fusion coefficients in the central region (nucleons are created with large momenta at small angles, $n=1$) and in the target-fragmentation region (moderate momenta, angular range $90°-180°$, $n=2$). For both regions there are predictions about the behavior of the fusion coefficients as functions of the mass numbers of the fragments and targets and the angular and momentum dependences. Dependence of the fusion coefficients only on k_- automatically arises in calculating the Feynman diagram of the process, where along with

the dependence of the fusion coefficient on k_- one also obtains the absolute value of the coefficient without free parameters. However, the calculated values of the fusion coefficients depend critically on the nature of the nuclear density distribution and on the values of the fragment radii. In an earlier study[84] the proportionality of the fusion coefficients in the deuteron to $1/k_-$ was obtained from purely geometrical considerations by analyzing the space-time picture of hadron–nucleus interactions.

The production of cumulative protons in hadron–nucleus interactions was studied in Ref. 85, where the contributions of various mechanisms (spectator, direct, and rescattering) to the inclusive cross sections were also calculated. The proton kinetic energies lie in the range 70–230 MeV for the angles 90°, 120°, and 160°. The results of the numerical calculations showed that rescattering dominates in the cross section at 90° and $T_p<160$ MeV. Above these energies the direct mechanism begins to dominate, and the contribution of the spectator mechanism is negligible. At 160° the main contribution comes from the spectator mechanism, and the contribution of the direct mechanism is negligible. The situation at 120° is not very clear because all mechanisms except the direct one are important.

Let us make a few remarks about cumulative proton production. For example, according to the data of the present study, the scaling variable x for protons in the momentum range studied (0.3–0.7 GeV/c) varies from 1.2 to 1.7. The scaling variable for pions in the same momentum range varies from 0.6 to 1.4. The proton cross sections significantly exceed the pion cross sections at the same values of the scaling variable. At the same time, the slope parameters of the proton and pion spectra are close in the hard part of the spectra. Protons are initially present in the nucleus as structural elements and can acquire a considerable energy via the various mechanisms mentioned above. There is a persistent idea that protons emitted into the backward hemisphere with momentum greater than 300 MeV/c, i.e., exceeding the average momentum of the Fermi motion, are cumulative. It is also known that there are at least two values of the slope parameter in the proton energy spectrum (for angles different from 180°). The results of the present study indicate that this limit should be moved up to 500 MeV/c, in order to tune out the complicated soft-proton production mechanism.

A more rigorous definition of the term "cumulative particle" is given in Ref. 86. It is based on isolating the kinematical region of variables where the quasiparticles characterizing the interaction dynamics are quarks. The criteria for this are $b_{ik}\geqslant 5$ and $x>1$, where

$$b_{ik}=-\left(\frac{p_i}{m_i}-\frac{p_k}{m_k}\right)^2. \tag{33}$$

The quantities b_{ik} are the squared differences of the 4-velocities, and p_i are the 4-momenta of the particles with mass m_i participating in the reaction. According to the notation of (4), in the frame of the fragmenting particle $b_{\mathrm{II,I}}=2T_{\mathrm{I}}/m_{\mathrm{I}}$, where T_{I} is the particle kinetic energy. The limits on the kinetic energy of the various particles are $T_\pi>0.35$ GeV, $T_K>1.23$ GeV, and $T_p>2.34$ GeV. The condition $b_{\mathrm{II,I}}>5$ implies that the energy per nucleon of the interacting nuclei must be greater than 4 GeV, beginning at which limiting fragmentation sets in. We see from these estimates that a proton kinetic energy satisfying both conditions has not been reached in the experiments performed so far. The ratios of the inclusive cross sections normalized to A as a function of x for various particles (K^+/π, K^+/K^-, $\pi^-/\bar{p}$; Ref. 87) differ in the regions $x<1$ and $x>1$; in the latter case they become constant (a different constant for each type of cross-section ratio). The ratios of the p/π cross sections grow in the entire range of x from 0.3 to 2.5. Therefore, in our opinion both theoretical work and future difficult experiments will be required to understand cumulative proton production.

The cluster model of cumulative particle production (the nuclear-fireball model) was developed in Refs. 88–92. A cluster is produced in the first collision of the primary particle with the nucleus. The resulting system is not a set of free particles, and over a period of time τ it behaves as a single hadronic system. In the cluster rest frame the time is $\tau\sim 1/m_\pi$. Subsequent collisions between the cluster and the intranuclear nucleons cause it to be in an excited state, the lifetime of which is τ_{rad} in the nuclear rest frame. The time between two successive collisions is $\Delta t=\lambda/v$, where λ is the mean free path of the cluster in the nucleus and v is the cluster velocity. The condition that the cluster not emit particles between two successive collisions is $\tau_{\mathrm{rad}}>\Delta t$ or

$$\frac{\tau_{\mathrm{rad}}}{(1-v^2)^{1/2}}>\lambda/v. \tag{34}$$

The cluster will emit secondary particles inside the nucleus when its velocity is decreased to the critical value $v_{\mathrm{cr}}=(1+\tau_{\mathrm{rad}}/\lambda)^{-1/2}$ owing to collisions with intranuclear nucleons. The spectrum of pions emitted by the cluster is given by

$$f(p,\vartheta)=\mathrm{const}\cdot\exp\left[-\frac{E-pv_{\mathrm{cr}}\cos\vartheta}{T_0(1-v_{\mathrm{cr}}^2)^{1/2}}\right], \tag{35}$$

where $p=|\mathbf{p}|$, $\vartheta=\vartheta(\mathbf{p}\cdot\mathbf{v})$, and T_0 is the universal hadron temperature $\simeq 160$ MeV. The characteristic "temperature" of the pion spectrum is

$$T_c=T_0[(1-v_{\mathrm{cr}})/(1+v_{\mathrm{cr}})]^{1/2}, \tag{36}$$

which can be estimated by choosing $\lambda\simeq(1-2)m_\pi^{-1}$. This corresponds to the velocity $v_{\mathrm{cr}}\simeq 0.7-0.8$, and therefore gives $T_c=67-53$ MeV, in good agreement with experiment.

In the case of emission of secondary protons, it is assumed that their appearance in the cumulative region is associated with the formation and decay of a fireball with nonzero baryon number. The spectrum of protons emitted by a baryonic fireball is given by

$$f(p,\vartheta)=\mathrm{const}\cdot\exp[-\gamma(E-vp\cos\vartheta)/T_B], \tag{37}$$

where E and p, as before, are the total energy and momentum of the secondary particles, $\gamma=(1-v^2)^{-1/2}$, and T_B is the fireball temperature. The values of v and T_B are determined from the experimental spectra at various fixed angles. In particular, the data on the reactions Ne+U (400 MeV/nucleon) and Au+Ar (500 MeV/nucleon) lead to the values $T_B\simeq 40-70$ MeV and $v=0.06-0.1$. The data obtained in the

process $\gamma+A\to p+X$ were described by (37). Analysis of the data for pions and protons at initial energy 400 GeV led to two values of the parameters T and v characterizing the spectra. For pions from tantalum nuclei the values are $T_\pi=148$ MeV and $v_\pi=0.63$. For protons they are $T_p=91$ MeV and $v_p=0.3$. The different values of the parameters for pions and protons might indicate the existence of two sources of particle emission.

Treatment of the fireball as a thermodynamical system corresponding to an ideal gas of quarks, antiquarks, and gluons (the quark–gluon plasma) leads to the following expression for the hadron spectra in fireball decay in its rest frame:

$$\phi=\exp\left[-\frac{(m^2+p^2)^{1/2}+\mu_h}{T}\right], \tag{38}$$

where the chemical potential of the hadron h is equal to the sum of the chemical potentials of its constituent quarks. For mesons, $\mu_m=\mu_{q1}-\mu_{q2}$. For baryons, $\mu_b=\mu_{b1}+\mu_{b2}+\mu_{b3}$. For nuclear matter with equal numbers of protons and neutrons containing u and d quarks, $\mu_u=\mu_d=\mu$ and $\mu_m=0$ (mesons), $\mu_b=3\mu$ (baryons). We see from (38) that the effect of the large proton mass is canceled by the nonzero value of μ_b. According to the model assumption, hadron–nucleus collisions occur via the production of a fireball containing the nucleons in the tube of nuclear matter lying on the path of the projectile with average values of the parameters T_b and v_b, and a fireball of zero baryon number with parameters T_m and v_m. The spectra of cumulative K^- and K^+ mesons are predicted to be different in this approach. The quark structure of the K^- meson is $(\bar{u},s)$ and that of the K^+ meson is $(u,\bar{s})$, and a K^- meson can be produced in a pair with a K^+ meson, the source of which is a fireball with the maximum temperature T and zero baryon number. There is an additional source of K^+ mesons due to the associated production of strange baryons (Λ, Σ, and so on). Here the creation of K^+ mesons is determined by the parameters T_b and v_b. The experimental data indicate that the yield of K^+ mesons is enhanced and that their A dependence is close to that for protons.[14,45]

Recent studies[93–97] reflect the current view of the problem of deep-inelastic processes on nuclei involving both leptons and hadrons. The experimental data are the results on cumulative particle production and deep-inelastic scattering (the BCDMS and EMC effects). As noted in Ref. 93, the discovered effects are in conflict with all (nonrelativistic) representations of the nucleus as a system of nucleons bound by potential forces. However, it turns out to be quite natural to view the nucleus as a relativistic, quantum-field bound system. The main feature of such a system is that owing to the vacuum polarization, the nucleus is not just a system of A interacting nucleons, but a particle–antiparticle sea carrying a certain fraction of the total nuclear momentum in the infinite-momentum frame. Here the momentum fraction of the nucleons must be decreased. In quark language this implies a decrease of the average momentum fraction of the valence quarks of the nucleus relative to that of a system of free nucleons. Quark models of cumulative particle production and the EMC effect are analyzed in Ref. 95.

Let us discuss the main points, following that study. The invariant cross section for the process $AB\to hX$ for a particle h in the fragmentation region of the nucleus A at small transverse momentum and neglecting the internal transverse motion of the quarks inside the nucleus has the form

$$\rho_{A\to h}(x,y,p_\perp)\equiv\varepsilon\frac{d\sigma}{d^3p_h}=\int_x^A f_h^B\left(\frac{x}{\alpha},y,p_\perp\right)F_A(\alpha)d\alpha, \tag{39}$$

where F_A is the nuclear structure function divided by the baryon number A, and f_h^B is some function whose form depends on the specific production mechanism of the hadron h, but is independent of the nucleus. For the mechanism of limiting fragmentation[1,3,8] the cross section is simply proportional to $F_A(x)$, i.e., $f_h^B(x/\alpha)\sim\delta(x/\alpha-1)$. Here $x=-u/s$ and $y=-t/s$.

In the classical potential picture of the nucleus, any structure function can be expressed in terms of the nucleon distribution in the nucleus T_A (determined by the one-nucleon wave function) and the nucleon structure function $F_N(x)$:

$$F_A(x,Q^2)=\int_x^A T_A(\alpha)F_N\left(\frac{x}{\alpha},Q^2\right)d\alpha. \tag{40}$$

The distribution T_A is normalized to conserve baryon number when F_A is taken to be the valence-quark distribution, and to conserve energy–momentum, when the combined distribution of all quarks, antiquarks, and gluons is used. Substitution of (40) into (39) gives the relation between the cross sections for processes on the nucleus and the nucleon:

$$\rho_{A\to h}(x,p_\perp)=\int_x^A T_A(\alpha)\rho_{N\to h}\left(\frac{x}{\alpha},p_\perp\right)d\alpha, \tag{41}$$

valid also for the cumulative region $x>1$. Few-nucleon correlations contribute to the high-momentum part ($\alpha>1$) of the function T_A, because the Fermi motion does not describe this part of the cumulative-particle spectrum. Studies of deep-inelastic scattering on nuclei show that the nuclear structure function does not reduce to the nucleon structure function, in the sense that there is no relation of the type (40) with a single function T_A for any distribution of quarks or gluons.

As was shown in Ref. 93, for a nucleus A and a nucleon there are in general relations of the type (41) with three independent distributions: one for the nonsinglet channel T_A^{NS} (valence quarks F_3), and two for the singlet channel $T_A^{\pm}$ (for the sum of the distributions of all the quarks and antiquarks F_2 and gluons G). Assuming that $T_A^+=T_A^-=T_A^S$ and that the integrals of T_A^S and T_A^{NS} differ by 4–6% for intermediate and heavy nuclei,

$$\int_0^A(T_A^S-T_A^{NS})d\alpha=\Delta_A\approx 0.04\text{–}0.06, \tag{42}$$

it is possible to obtain an excellent quantitative description of the ratio of the structure functions in the entire experimental range of x. Attainment of this value of the EMC effect for valence quarks in the region $x>0.4$ requires that

$$\int_0^A (1-\alpha)T_A^{NS}(\alpha)d\alpha = \int_0^A \alpha(T_A^S(\alpha)-T_A^{NS}(\alpha))d\alpha \simeq \Delta_A , \tag{43}$$

i.e., the total momentum of the "valence" nucleons must be smaller than the nucleus momentum. Owing to the differences in (42) and (43), the nucleus must contain, in addition to the $q\bar{q}$ and gluon seas of the valence nucleons, a "collective" sea of $q\bar{q}$ pairs which is small in magnitude ($\sim\Delta_A$) but just as hard as the valence-quark distribution.

The difference between T_A^S and T_A^{NS} leads to a new element in nuclear structure: an additional collective nuclear quark–antiquark and gluon sea. Despite the smallness of the parameter Δ_A, it has just as hard a distribution spectrum as do the valence quarks, which can play a decisive role in the spectrum of cumulative K^- and $\bar{p}$ not containing valence quarks of the nucleus. In the region $x>1$ their spectrum must be completely determined by the additional sea, owing to the more rapid falloff of the nucleon contribution. The study of these particles reveals an interesting possibility for understanding the nature of the difference between the nucleus and nucleon structure functions. This difference may arise owing to rescattering of valence and sea quarks in multiquark fluctons. Then in the region $x\simeq 1$, where the contribution of the multiquark component to the valence-quark distribution is still small and the contribution of the antiquarks of the collective sea dominates, the yield ratio $K^+/K^-\simeq u_A(x)/\bar{u}_A(x)$ will depend weakly on x and will amount to $\simeq 2/\Delta_A \approx 30-40$ for intermediate and heavy nuclei. In the region $x\simeq 2$, where multiquark fluctons begin to dominate also in the valence part, this ratio must decrease to $2/\Delta_2 \simeq 4-6$. If the valence and sea quarks are redistributed throughout the entire nucleus either as a result of rescattering on each nucleon or owing to transfer of part of the nucleon momentum into certain meson or $N\bar{N}$ components, this falloff should not occur.

According to this approach, cumulative production of antiprotons can give information about the possible packing of the collective sea. If it is packed with $N\bar{N}$ pairs, the main mechanism for antinucleon production must be antidiquark fragmentation, and a large ratio $\bar{p}/p\approx\Delta_A/2$ should be expected. If there is no such packing, the dominant mechanism is fragmentation of an antiquark of the nuclear sea into an antiproton, which leads to additional suppression of the antiproton yield.

A new approach to the description of cumulative particle production on the basis of the quark–gluon string model is described in Refs. 96 and 97. The model gives a more successful description of the fragmentation of ordinary hadrons, assuming the existence of heavy multiquark states in the fragmenting nuclei. The main problem is to explain the cumulative production of particles of the type K^- and $\bar{p}$, which contain only sea quarks. An interesting experimental fact, mentioned above, is that the ratios of the yields of these particles to the yields of particles which are similar but contain valence quarks of the nucleus are independent of x for $x>1$. In the case of nucleon fragmentation the yield ratio falls sharply as a function of x. This behavior cannot be explained by the simplest fragmentation models using the valence- and sea-quark distributions measured in deep-inelastic scattering, or by models of nuclei consisting of nucleons. The reason is that the distribution of sea quarks in the nucleon falls off rapidly compared with that of valence quarks. The difference between these distributions is much smaller in the quark–gluon string model. It was shown in Refs. 96 and 97 that the difference is too small to obtain approximately constant behavior of the K^+/K^- ratio as a function of x, without coming into contradiction with the experimental data from nucleon–nucleon scattering. Analysis of the spectra of cumulative K^+ and K^- mesons has shown that they are similar and consistent with the available experimental data.[21,24] The model predicts growth of the $K^-/\bar{p}$ yield ratio as a function of x in hadron–nucleus interactions.

The theoretical approaches to the problem of cumulative particle production can arbitrarily be characterized as either hot or cold. These terms reflect the conditions under which a source of cumulative particles (fluctons, few-nucleon correlations, fireballs, clusters, and so on) appears. Hot models start from the assumption that such an object arises in the interaction process and then decays into particles with certain characteristics. Cold models presuppose the existence of such an object in the initial (fragmenting) nucleus with no dependence on the initial particle.

We see that none of the models considered gives a comprehensive explanation of all the characteristics of cumulative particle production or, even more so, of the details in the behavior of the cross sections. Nevertheless, all these models explain the main properties of cumulative production with some degree of success. Not all the model predictions agree with the available experimental data, and some require additional experimental information. The common feature of the theoretical approaches is the use of non-nucleon degrees of freedom, especially for particles consisting of sea quarks.

THE MAIN RESULTS

1. Using a single experimental procedure, we have made the first detailed study of the A dependence of the cross sections for cumulative particle production in proton and nucleus beams in a wide range of fragmenting nuclei from deuterium to lead, and have shown that these dependences scale. In addition, we have discovered detailed scaling in the behavior of the cross sections on isotopically enriched nuclei, which is manifested for all the beams used.

TABLE IX. $p(4.5\ \text{GeV}/c)+A$, $\vartheta=120°$, $\mathbf{p}=0.5\ \text{GeV}/c$.

A	d	p	$\pi^+(\times 10^{-1})$	$\pi^-(\times 10^{-1})$
^{6}Li	0.212±0.004	1.47±0.03	0.58±0.012	0.48±0.01
C	0.67±0.02	3.02±0.06	0.65±0.013	0.66±0.013
Si	1.25±0.03	4.63±0.09	0.85±0.017	0.73±0.014
^{58}Ni	2.04±0.04	6.23±0.13	0.85±0.017	0.70±0.014
^{64}Ni	2.10±0.04	5.68±0.11	0.76±0.015	0.78±0.016
^{64}Zn	2.08±0.04	6.02±0.12	0.79±0.016	0.70±0.014
^{114}Sn	2.39±0.05	6.37±0.13	0.69±0.014	0.65±0.013
^{124}Sn	2.39±0.05	5.66±0.11	0.62±0.012	0.70±0.014
Pb	3.18±0.06	6.43±0.12	0.57±0.011	0.59±0.012

TABLE X. D(4.5 GeV/c)+A, $\vartheta = 120°$, $\mathbf{p} = 0.5$ GeV/c.

A	d	p	$\pi^+(\times 10^{-1})$	$\pi^-(\times 10^{-1})$
D		0.42±0.012	0.228±0.006	0.241±0.006
^{4}He	0.334±0.009	2.26±0.07	0.890±0.018	0.93±0.02
^{6}Li	0.344±0.007	2.24±0.05	0.848±0.017	0.76±0.04
C	1.12±0.02	4.97±0.1	1.21±0.02	1.08±0.12
Si	2.05±0.04	6.99±0.14	1.29±0.03	1.28±0.12
^{58}Ni	3.74±0.07	9.8±0.2	1.27±0.03	1.17±0.04
^{64}Ni	3.73±0.12	8.87±0.3	1.16±0.02	1.31±0.03
^{64}Zn	3.92±0.08	9.9±0.2	1.24±0.02	1.15±0.03
^{114}Sn	4.72±0.09	10.5±0.2	1.08±0.02	1.10±0.02
^{124}Sn	4.90±0.09	9.67±0.19	0.98±0.02	1.13±0.05
Pb	6.32±0.13	11.0±0.2	0.94±0.03	0.95±0.02

TABLE XI. He(4.5 GeV/c)+A, $\vartheta = 120°$, $\mathbf{p} = 0.5$ GeV/c.

A	d	p	$\pi^+(\times 10^{-1})$	$\pi^-(\times 10^{-1})$
^{6}Li	0.302±0.016	2.16±0.05	0.783±0.029	0.746±0.041
C	1.17±0.02	6.08±0.12	1.63±0.04	
Si	2.13±0.06	7.24±0.14	1.30±0.06	1.13±0.07
^{58}Ni	3.65±0.07	10.2±0.2	1.41±0.05	1.05±0.08
^{64}Ni	3.95±0.08	9.6±0.2	1.41±0.05	1.33±0.10
^{64}Zn	3.98±0.08	10.6±0.2	1.54±0.05	1.26±0.07
^{114}Sn	5.62±0.11	11.6±0.2	1.32±0.04	1.22±0.05
^{124}Sn	5.51±0.11	10.6±0.2	1.23±0.05	1.28±0.05
Pb	7.6±0.3	12.9±0.3	1.17±0.02	1.11±0.03

TABLE XII. C(4.5 GeV/c)+A, $\vartheta = 120°$, $\mathbf{p} = 0.5$ GeV/c.

A	d	p	$\pi^+(\times 10^{-1})$	$K^+(\times 10^{-1})$
^{6}Li	0.66±0.02	4.77±0.09	1.84±0.05	0.104±0.061
^{7}Li	0.81±0.06	4.97±0.09	2.20±0.11	0.28±0.13
C	1.81±0.04	10.21±0.42	3.18±0.04	0.15±0.04
Al	3.42±0.08	14.08±0.28	3.45±0.06	0.16±0.034
Cu	7.84±0.14	22.3±1.0	3.89±0.06	0.35±0.05
^{114}Sn	10.6±0.3	25.22±0.35	3.4±0.2	0.29±0.17
^{119}Sn	10.6±0.24	24.6±0.5	3.43±0.07	0.52±0.08
Pb	11.9±0.5	25.91±0.35	3.17±0.12	0.39±0.04

TABLE XIII. $B+A \to K^+ + \ldots$, $\vartheta = 120°$, $\mathbf{p} = 0.5$ GeV/c.

	B			
A	p $(\times 10^{-3})$	D $(\times 10^{-3})$	^{4}He $(\times 10^{-3})$	C $(\times 10^{-2})$
D		0.16±0.08		
^{4}He		0.91±0.22		
^{6}Li	0.53±0.19	1.0±0.3	2.0±1.3	1.0±0.6
^{7}Li				2.8±1.3
C	0.70±0.22	2.2±0.3	3.0±0.9	1.5±0.4
Al				1.6±0.3
Si	3.0±0.5	4.3±0.7	3.9±2.0	
^{58}Ni	2.7±0.7	7.4±1.0	3.2±1.9	
^{64}Ni	2.0±0.9	7.2±1.2	8.0±3.7	
^{64}Zn	3.0±0.5	6.5±0.9	9.9±3.0	
Cu				3.5±0.5
^{114}Sn	3.0±0.5	6.9±1.0	11±3	2.9±1.7
^{119}Sn				5.2±0.8
^{124}Sn	3.7±0.8	8.2±0.9	13±6	
Pb	2.6±0.8	12±4	12±2	3.9±0.4

TABLE XIV. p(8.9 GeV/c)+A, $\vartheta = 120°$, $\mathbf{p} = 0.5$ GeV/c.

A	K^+ $(\times 10^{-2})$	K^- $(\times 10^{-4})$
^{58}Ni	1.22±0.05	2.9±0.7
^{64}Ni	1.19±0.05	3.6±1.0
^{4}Zn	1.32±0.03	3.2±0.7
^{114}Sn	1.59±0.05	3.9±0.4
^{124}Sn	1.48±0.06	3.0±0.5
Pb	1.25±0.18	

TABLE XV. p(8.9 GeV/c)+A; $\vartheta = 120°$, $\mathbf{p} = 0.3$ GeV/c.

A	p	π^+	π^-
^{58}Ni	61.0±1.2	1.43±0.06	1.05±0.02
^{64}Ni	57.6±1.2	1.30±0.04	1.10±0.02
^{64}Zn	59.7±1.2	1.49±0.03	1.09±0.02
^{114}Sn	69.3±1.4	1.38±0.03	0.985±0.020
^{124}Sn	57.3±1.2	1.22±0.02	0.971±0.020
Pb	77.3±1.5	1.20±0.04	0.907±0.019

TABLE XVI. $p(8.9\ \text{GeV}/c)+A$, $\vartheta=120°$, $\mathbf{p}=0.4$ GeV/c.

A	p	π^+ $(\times10^{-1})$	π^- $(\times10^{-1})$
^{58}Ni	18.8±0.04	4.30±0.10	3.03±0.07
^{64}Ni	17.1±0.3	3.81±0.12	3.27±0.07
^{64}Zn	19.3±0.4	4.30±0.10	3.24±0.06
^{114}Sn	22.2±0.4	3.75±0.09	3.06±0.06
^{124}Sn	18.9±0.4	3.44±0.08	2.91±0.06
Pb	25.0±0.6	3.35±0.07	2.90±0.06

TABLE XVII. $p(8.9\ \text{GeV}/c)+A$, $\vartheta=120°$, $\mathbf{p}=0.5$ GeV/c.

A	d	p	π^+ $(\times10^{-1})$	π^- $(\times10^{-1})$
^{58}Ni	2.33±0.05	5.39±0.11	1.11±0.03	0.91±0.03
^{64}Ni	2.41±0.05	5.12±0.10	1.00±0.02	0.99±0.03
^{64}Zn	2.36±0.05	5.88±0.12	1.16±0.03	0.91±0.05
^{114}Sn	3.46±0.07	6.82±0.14	0.98±0.02	0.93±0.02
^{124}Sn	3.13±0.06	6.03±0.12	0.88±0.02	0.97±0.02
Pb	4.50±0.09	7.22±0.14	0.88±0.03	0.93±0.02

TABLE XVIII. $p(8.9\ \text{GeV}/c)+A$, $\vartheta=120°$, $\mathbf{p}=0.6$ GeV/c.

A	d	p	π^+ $(\times10^{-2})$	π^- $(\times10^{-2})$
^{58}Ni	0.82±0.02	1.73±0.04	3.00±0.07	2.41±0.06
^{64}Ni	0.84±0.02	1.60±0.03	2.75±0.06	
^{64}Zn	0.86±0.02	1.78±0.04	2.95±0.07	2.61±0.07
^{114}Sn	1.24±0.03	2.05±0.04	2.84±0.12	2.51±0.06
^{124}Sn	1.15±0.03	1.82±0.05	2.50±0.06	2.57±0.06
Pb	1.69±0.04	2.25±0.05	2.66±0.08	2.60±0.06

TABLE XIX. $p(8.9\ \text{GeV}/c)+A$, $\vartheta=120°$, $\mathbf{p}=0.7$ GeV/c.

A	d $(\times10^{-1})$	p $(\times10^{-1})$	π^+ $(\times10^{-3})$	π^- $(\times10^{-3})$
^{58}Ni	2.85±0.06	4.97±0.11	7.30±0.30	5.95±0.24
^{64}Ni	2.87±0.06	4.68±0.09	6.34±0.21	6.58±0.25
^{64}Zn				6.36±0.25
^{114}Sn	4.53±0.11	6.22±0.12	6.92±0.25	6.20±0.20
^{124}Sn	4.07±0.08	5.44±0.11	5.94±0.16	6.40±0.20
Pb	5.90±0.15	6.60±0.10	6.30±0.20	6.56±0.21

TABLE XX. Parameters of the approximation of the energy dependence of the proton cross sections for p momentum in the range 0.3–0.5 GeV/c.

A	T_0	B_T	χ^2/n.d.f.
^{58}Ni	32.3±0.4	252±8	13
^{64}Ni	32.5±0.4	231±8	30
^{64}Zn	33.8±0.4	231±8	14
^{114}Sn	33.8±0.4	267±9	18
^{124}Sn	34.9±0.4	211±7	17
Pb	33.0±0.4	313±10	6

TABLE XXI. Parameters of the approximation of the energy dependence of the proton cross sections for p momentum in the range 0.5–0.7 GeV/c.

A	T_0	B_T	χ^2/n.d.f.
^{58}Ni	45.0±0.6	86±4	1.0
^{64}Ni	44.9±0.5	81±4	2.4
^{64}Zn	42.3±1.0	113±10	1.0
^{114}Sn	45.0±0.5	107±5	10
^{124}Sn	44.7±0.5	97±5	5
Pb	44.9±0.5	115±5	2.4

TABLE XXII. Parameters of the approximation of the dependence of the proton cross sections on the cumulative number x for p momentum in the range 0.3–0.5 GeV/c.

A	x_0	B_x	χ^2/n.d.f.
^{58}Ni	0.093±0.001	781±36	1.4
^{64}Ni	0.094±0.001	718±33	8
^{64}Zn	0.098±0.001	681±31	2
^{114}Sn	0.098±0.001	788±36	3
^{124}Sn	0.101±0.001	605±28	3
Pb	0.096±0.001	941±43	10

TABLE XXIII. Parameters of the approximation of the dependence of the proton cross sections on the cumulative number of x for p momentum in the range 0.5–0.7 GeV/c.

A	x_0	B_x	χ^2/n.d.f.
^{58}Ni	0.115±0.001	313±21	1.0
^{64}Ni	0.114±0.001	300±19	1.0
^{64}Zn	0.110±0.003	408±50	1.0
^{114}Sn	0.114±0.001	394±25	4.6
^{124}Sn	0.114±0.001	359±23	2.0
Pb	0.114±0.001	422±27	1.0

TABLE XXIV. Parameters of the approximation of the dependence of the proton cross sections on the light-front variable α for p momentum in the range 0.3–0.5 GeV/c.

A	α_0	B_α	χ^2/n.d.f.
^{58}Ni	0.078±0.001	872±41	1.0
^{64}Ni	0.078±0.001	802±38	6.0
^{64}Zn	0.082±0.001	756±35	1.0
^{114}Sn	0.082±0.001	875±41	2.0
^{124}Sn	0.084±0.001	671±32	2.0
Pb	0.080±0.001	1047±49	1.0

TABLE XXV. Parameters of the approximation of the dependence of the proton cross sections on the light-front variable α for p momentum in the range 0.5–0.7 GeV/c.

A	α_0	B_α	χ^2/n.d.f.
^{58}Ni	0.093±0.001	398±28	1.0
^{64}Ni	0.092±0.001	381±25	1.0
^{64}Zn	0.090±0.002	501±64	1.0
^{114}Sn	0.092±0.001	502±34	3.0
^{124}Sn	0.092±0.001	457±30	1.0
Pb	0.092±0.001	537±35	1.0

TABLE XXVI. Parameters of the approximation of the energy dependence of the π^+ cross sections for π^+ momentum in the range 0.3–0.7 GeV/c.

A	T_0	B_T	χ^2/n.d.f.
^{58}Ni	72.4±0.6	21.0±0.1	1.6
^{64}Ni	72.5±0.5	18.8±0.8	3.6
^{64}Zn	72.8±0.5	21.0±0.7	1.1
^{114}Sn	72.4±0.5	19.0±0.6	1.8
^{124}Sn	72.3±04	17.3±0.5	2.7
Pb	73.6±0.5	16.0±0.6	3.0

TABLE XXVII. Parameters of the approximation of the energy dependence of the π^- cross sections for π^- momentum in the range 0.3–0.5 GeV/c.

A	T_0	B_T	χ^2/n.d.f.
^{58}Ni	76.5±1.0	12.7±0.7	1.6
^{64}Ni	78.0±1.0	12.8±0.6	1.0
^{64}Zn	75.8±1.0	13.7±0.7	1.0
^{114}Sn	79.6±1.0	11.0±0.5	2.4
^{124}Sn	86.6±2.0	7.8±0.7	1.0
Pb	82.7±1.0	9.1±0.4	1.0

TABLE XXVIII. Parameters of the approximation of the energy dependence of the π^- cross sections for π^- momentum in the range 0.5–0.7 GeV/c.

A	T_0	B_T	χ^2/n.d.f.
^{58}Ni	71.5±1.0	19.0±2.0	1.0
^{64}Ni	71.8±1.3	19.0±2.0	1.2
^{64}Zn	74.0±1.3	16.0±1.7	4.7
^{114}Sn	72.4±1.0	18.0±1.5	1.7
^{124}Sn	71.8±1.0	19.0±1.6	1.0
Pb	73.8±1.0	16.0±1.4	2.3

TABLE XXIX. Parameters of the approximation of the dependence of the π^+ cross sections on the cumulative number x for π^+ momentum in the range 0.3–0.7 GeV/c.

A	x_0	B_x	χ^2/n.d.f.
^{58}Ni	0.149±0.001	78±4	1.0
^{64}Ni	0.150±0.001	69±3	1.8
^{64}Zn	0.149±0.001	82±4	1.0
^{114}Sn	0.149±0.001	73±3	4.8
^{124}Sn	0.149±0.001	65±2	3.2
Pb	0.152±0.001	57±3	3.3

TABLE XXX. Parameters of the approximation of the dependence of the π^- cross sections on the cumulative number x for π^- momentum in the range 0.3–0.5 GeV/c.

A	x_0	B_x	χ^2/n.d.f.
^{58}Ni	0.155±0.002	48±4	2.5
^{64}Ni	0.157±0.002	48±3	1.7
^{64}Zn	0.153±0.002	53±4	1.5
^{114}Sn	0.161±0.002	39±2	1.0
^{124}Sn	0.176±0.002	24±3	1.0
Pb	0.167±0.002	31±2	1.1

TABLE XXXI. Parameters of the approximation of the dependence of the π^- cross sections on the cumulative number x for π^- momentum in the range 0.5–0.7 GeV/c.

A	x_0	B_x	χ^2/n.d.f.
^{58}Ni	0.150±0.003	60±9	1.0
^{64}Ni	0.151±0.003	62±8	1.0
^{64}Zn	0.155±0.002	50±6	3.0
^{114}Sn	0.152±0.002	57±6	1.0
^{124}Sn	0.151±0.002	62±6	1.0
Pb	0.155±0.002	50±5	1.0

TABLE XXXII. Parameters of the approximation of the dependence of the π^+ cross sections on the light-front variable α for π^+ momentum in the range 0.3–0.7 GeV/c.

A	α_0	B_α	χ^2/n.d.f.
^{58}Ni	0.117±0.001	121±7	2.0
^{64}Ni	0.118±0.001	106±6	4.0
^{64}Zn	0.118±0.001	115±5	1.8
^{114}Sn	0.117±0.001	107±5	1.4
^{124}Sn	0.117±0.001	97±4	3.0
Pb	0.119±0.001	88±4	3.1

TABLE XXXIII. Parameters of the approximation of the dependence of the π^- cross sections on the light-front variable α for π^- momentum in the range 0.3–0.5 GeV/c.

A	α_0	B_α	χ^2/n.d.f.
^{58}Ni	0.125±0.002	63±5	1.1
^{64}Ni	0.127±0.002	62±4	1.0
^{64}Zn	0.124±0.002	69±5	1.0
^{114}Sn	0.130±0.001	51±3	1.0
^{124}Sn	0.140±0.003	33±4	1.0
Pb	0.135±0.002	40±3	1.0

TABLE XXXIV. Parameters of the approximation of the dependence of the π^- cross sections on the light-front variable α for π^- momentum in the range 0.5–0.7 GeV/c.

A	α_0	B_α	χ^2/n.d.f.
^{58}Ni	0.115±0.002	112±1	1.0
^{64}Ni	0.116±0.002	117±1	1.0
^{64}Zn	0.119±0.002	90±1	4.9
^{114}Sn	0.117±0.002	104±1	1.9
^{124}Sn	0.116±0.001	115±1	1.0
Pb	0.119±0.002	91±1	2.5

TABLE XXXV. Parameters of the approximation of the dependence of the deuteron cross sections in various representations for d momentum in the range 0.5–0.7 GeV/c.

A	T_0	B_T	χ^2/n.d.f.
^{58}Ni	29.0±0.4	22.0±1	7.0
^{64}Ni	28.6±0.4	23.0±1	6.0
^{64}Zn	27.9±0.9	25.0±2	1.0
^{114}Sn	29.8±0.5	30.0±1	9.0
^{124}Sn	29.9±0.4	28.0±1	4.0
Pb	29.9±0.5	40.0±2	2.0

TABLE XXXVI. Parameters of the approximation of the dependence of the deuteron cross sections in various representations for d momentum in the range 0.5–0.7 GeV/c.

A	x_0	B_x	χ^2/n.d.f.
^{58}Ni	0.101±0.001	111±8	1.0
^{64}Ni	0.100±0.001	121±8	1.0
^{64}Zn	0.101±0.003	113±1	1.5
^{114}Sn	0.104±0.002	146±1	3.0
^{124}Sn	0.104±0.001	134±9	1.0
Pb	0.104±0.002	191±1	1.0

TABLE XXXVII. Parameters of the approximation of the dependence of the deuteron cross sections in various representations for d momentum in the range 0.5–0.7 GeV/c.

A	α_0	B_α	χ^2/n.d.f.
^{58}Ni	0.081±0.001	139±1	1.0
^{64}Ni	0.080±0.001	151±1	1.0
^{64}Zn	0.082±0.003	135±1	1.0
^{114}Sn	0.084±0.001	181±1	2.0
^{124}Sn	0.084±0.001	166±1	1.0
Pb	0.084±0.001	236±1	1.0

2. We have performed the first detailed investigation of the energy dependence of the cross sections on isotopically enriched nuclei of nickel, zinc, and tin, using an 8.9-GeV/c proton beam, and we have determined the values of the slope parameters in the representations traditional in the study of cumulative processes. The A dependence of the secondary-particle cross sections has been studied in just as great detail in the momentum range 0.3–0.7 GeV/c. The wide range of fragmenting nuclei made it possible to reveal the characteristic features of different subranges of nuclei.

3. We have discovered a correlation between the cross sections and the nuclear density for light nuclei (D, He, ^{6}Li, ^{7}Li, C). It is this which is mainly responsible for the sharp increase in and irregularities of the behavior of the cross sections in this range of nuclei. The data for emission angle 180° indicate the same behavior of the cross sections in this range of nuclei. The π^+/π^- and p/π^+ cross-section ratios on light (^{6}Li) and heavy (Pb) nuclei are independent of the mass number of the projectile nucleus. The π^+/π^- cross-section ratios are close in magnitude for light and heavy nuclei, while the ratio of neutrons and protons in Pb is 1.5.

4. For intermediate and heavy nuclei we have discovered an isotopic effect in the behavior of the cross sections: the production cross section of positively charged particles (π^+,K^+,p) is independent of the neutron excess at fixed nuclear charge. On the other hand, the cross section for π^- production is correlated with the neutron excess. The two effects occur in proton, deuteron, and He beams. These effects are comparable in magnitude to the relative proton and neutron contents in the fragmenting nuclei.

5. On light nuclei ^{6}Li and ^{7}Li the isotopic effect is manifested only for π^+ mesons in proton–nucleus interactions. The isotopic effect is absent in beams of carbon nuclei: the production cross sections for positively charged particles π^+, K^+, and p grow in going from ^{6}Li to ^{7}Li.

6. The ratios of the structure functions (ratios of the inclusive cross sections) on isotopically enriched nuclei as a function of the scaling variable x demonstrate symmetric behavior for pions of different sign of the charge, owing to the relative proton and neutron contents in the nuclei. The analogous cross-section ratios for protons on the same nuclei reveal a marked x dependence in the soft (up to 0.5 GeV/c) part of the spectrum, especially in the case of tin isotopes.

7. Comparison of the cross sections of positively and negatively charged particles on fragmenting nuclei which are isobars (^{64}Zn and ^{64}Ni) shows that the nuclear charge plays the dominant role in the production of positive particles.

8. The isotopic effect in the behavior of the cross sections for π^+, π^-, and p is manifested in the same manner in primary proton beams of momentum 4.5 GeV/c and 8.9 GeV/c.

9. The exponents of the A dependence of the cross sections for pions, protons, and deuterons as functions of the mass number of the primary beams demonstrate scaling behavior, increasing in magnitude as the type of beam changes. Beginning with beams of He nuclei they become constant, a different constant for each particle.

CONCLUDING REMARKS

We have considered processes of cumulative particle production in interactions of nuclear beams with a large group of fragmenting nuclei, essentially encompassing the entire periodic table. Comparison with the results of studies for beams of various types of particles at various energies shows that the main features of cumulative production are to a large degree preserved and, in some cases, even preserved in detail. It has been found that for studying the details in the behavior of the cross sections for cumulative particles, the most sensitive characteristic is the A dependence of the cross sections, which is manifested specifically in various regions of fragmenting nuclei.

The A dependences of the cross sections on proton and nucleus beams were measured in this study at a secondary-particle momentum of 0.5 GeV/c, which corresponds to the scaling variable $x \simeq 1$ for pions. In Refs. 45 and 98 the A dependence of the pion cross sections was studied for $x = 1.3$ and 2.1. The measurements were made at different emission angles (90° and 168°) using more than 20 nuclei and demonstrated the scaling behavior of the cross sections.

The results of the present work were obtained by studying inclusive processes with the maximum possible specification of the initial state, which pertains to the type of fragmenting nuclei chosen. The statistical errors in the measurement of the cross sections are 2–5% in most cases. It is these facts which have set the terms for the detailed studies. The detailed scaling in the behavior of the cross sections both for the A dependence on proton and nucleus beams and for the energy dependence of the cross sections on proton beams with twice the momentum is a weighty argument in favor of a single mechanism for the evolution of the interaction process leading to the production of cumulative particles, at least under the kinematical conditions of the present study. The A dependence of the cross sections measured at fixed momentum of the observed particles demonstrates scaling behavior as a function of the nuclear density for light nuclei, independently of the sign of the particle charge. For intermediate nuclei the sign of the particle charge is correlated with the relative proton and neutron content. This correlation vanishes for heavy nuclei. Therefore, three regions of fragmenting nuclei are distinguished, each one interesting in itself. Identical momentum of the particles in the study of the A dependence is the only common feature. Secondary particles of different masses possess different kinetic energies and suggest that the properties of detailed scaling are preserved when their kinetic energies or initial momenta are changed. This has proved to be true for primary proton beams (at values of the momentum differing by a factor of two).

The set of results obtained in the present study represents new experimental material for studying processes of cumulative particle production in beams of protons and nuclei. The secondary-particle spectrum contains both the structural elements of the nuclei and structures arising in the interaction. The detailed scaling in the behavior of the cross sections of particles differing so greatly in their kinematical and quantum characteristics may be related to the specific behavior of the nuclear medium in the case of isotopically enriched nuclei or to the effect of the electromagnetic field of the incident particle on the initial state of the fragmenting nucleus. It is also possible that both factors play a role.

The correlation with the nuclear density, which varies maximally for light nuclei, may be the decisive reason for the existence of configurations which generate cumulative particles. Of course, correlations on this scale are not observed in the region of nuclei where the density is approximately constant. The variable quantity in this region of nuclei is the charge density, due to the variation of the nuclear charge radii. The estimates given above indicate a possible correlation between the cross sections and the charge density. Since a correlation with the neutron content is observed in π^- production, it could be assumed, as for positively charged particles, that there is a relation between the cross sections and the neutron-distribution density. However, in this case there is no experimentally known characteristic such as the rms radius, so that we can only hypothesize. On the other hand, it can be assumed that the protons and neutrons of the nucleus are not uniformly distributed from the viewpoint of the incident particle, which via its own electromagnetic field can interact earlier and more strongly with the charged protons (more precisely, with the region occupied by the nuclear charge, since some neutrons necessarily participate in forming this region). This can induce polarization of the nuclear medium, which, in turn, can lead to spatial separation of the sources emitting particles of different sign of the electric charge.

The fact that the cross sections for cumulative particles on nuclei with different neutron content but identical charge (equal to the number of protons) behave differently shows that the initial states of the nuclei make a definite contribution to the interaction process, while the contribution from the incident particles is leveled out, because the isotopic effect is the same for different beams. However, in all cases we have beams of charged particles, and it would be interesting to perform an experiment to study these effects using primary beams of neutral particles, for example, neutrons from the stripping of deuterons.

We think that it would be interesting to study the behavior of the cross sections of sea particles (K^- and $\bar{p}$) for the group of nuclei ^{58}Ni, ^{64}Ni, and ^{64}Zn even in an inclusive experiment, in order to determine the scale of the isotopic effect or its absence for such particles.

The near equality of the π^+ and π^- cross sections on nuclei with neutron content significantly greater than the proton content is a well established fact and has been noticed in the studies cited above. A possible explanation is that a neutron halo exists at the periphery of the nucleus, where a significant number of neutrons can be concentrated. This would affect their density distribution. Regarding this, there are some interesting data obtained in experiments using radioactive beams.[99] For example, the ^{11}Li nuclei produced experimentally have size comparable to that of the Pb nucleus, but they are nevertheless a bound system in which the "extra" neutrons are pushed out to the periphery of the nucleus. These experiments have revealed interesting features in the nuclear structure related to the neutron and proton excesses.

The results of the present study give well defined guidlines for performing correlation experiments. The region of fragmenting nuclei, the type and energy of the primary beams and secondary particles, and the emission angles can be fairly arbitrary. Accordingly, different regions of values of the scaling variables can be chosen. The types of correlation can be rather diverse, beginning from measurement of the hadronic accompaniment for a particular cumulative particle, to study of the interference of identical particles, as has been done, for example, in the studies by the ITEP group[100] on nuclei with natural isotope content.

A relativistically invariant approach to the description of multiparticle processes in the space of relative 4-velocities $b_{ik}=-(u_i-u_k)^2$ has been developed in a series of studies[101-107] and applied to a large set of experimental data. Here $u_i=P_i/m_i$ is the hadron 4-momentum divided by its mass. The indices i,k take the values I,II,1,2, ... when the inclusive process is written as $\mathrm{I}+\mathrm{II}\to 1,2,\ldots+X$. The invariant cross section for the production of n particles is treated as a distribution function in the space of the b_{ik}: $F(b_{\mathrm{I\,II}},b_{\mathrm{I}1},b_{\mathrm{I}2},\ldots,b_{\mathrm{II}1},b_{\mathrm{II}2},\ldots,b_{12},\ldots)$. The function F is monotonic in these variables and falls off sufficiently rapidly for $b_{ik}\to\infty$. This property of F is manifested as the correlation-depletion principle, allowing the hadrons to be defined as clusters of partons with small relative velocities b_{ik}, and deconfinement to be defined as a process giving rise to particles with $b_{ik}\gg 5$.

A new approach to the study of correlation phenomena in multiple-production processes was suggested in Ref. 102. For example, the expression for the correlation function of any three particles 1,2,3 is

$$C_3=W(b_{12},b_{13},b_{23})-W(b_{12})W(b_{13})W(b_{23}). \qquad (44)$$

Here $W(b_{12})$, $W(b_{13})$, and $W(b_{23})$ are the one-dimensional distributions in the variables b_{12}, b_{13}, and b_{23}, and $W(b_{12},b_{13},b_{23})$ is the three-dimensional distribution in the same variables. These and the other distributions are taken from experiment. Specific expressions for different forms of the correlation functions are given in Ref. 102.

Particle multiple production has been analyzed in the space of relative velocities for the reaction $\pi^-(40\ \mathrm{GeV}/c)+\mathrm{C}\to\pi^\pm+X$ (in a propane chamber). The distributions of pion pairs in b_{ik} turned out to be identical in the fragmentation regions of the pion beam and the C nucleus. The analogous dependences for $\pi^\pm$ mesons and protons in the target fragmentation region differ significantly in the values of b_{ik}, in particular, the values of $b_{\mathrm{II}1}$. The properties of pion jets expressed in these variables turned out to be similar in $\pi^-\mathrm{C}$ interactions in both the pion fragmentation region and the target fragmentation region. Studies of the proton distributions in pC, dC, CC, pTa, and dTa interactions (4 GeV/nucleon) and $\pi^-\mathrm{C}$ interactions (40 GeV/c) (Ref. 103) revealed the presence of 4-dimensional baryon clusters whose properties are independent of the type and energy of the projectile. It was also shown that in relativistic nuclear reactions there are two regions characterized by different values of b_{ik}. Values $b_{ik}\sim 10^{-2}$ correspond to classical nuclear-physics processes, and values $b_{ik}\sim 10^{-1}$ correspond to the transition region, where the quark–gluon degrees of freedom are included.

We have sketched only the general aspects of the problem. The possibilities offered by the use of the space of variables b_{ik} and the justification of self-similarity and correlation depletion in interactions of various objects with nuclei in a wide range of energies are given in the studies cited, which include the details of the determination of the jet axis, the cluster center, and so on. All these questions are treated more systematically and completely in Ref. 107.

The next-generation SPHERE installation[108] offers great possibilities for further study. This installation is designed to study multiple cumulative particle production in nearly 4π geometry. Among the main goals are the following:

(1) Study of reactions producing two or more particles (π, K, p, $\bar{p}$,...) and vector-meson (ρ,ϕ,ω) production in the cumulative region; searching for narrow resonances due to the manifestation of hidden color, exotic quark states, and resonance quark (multiquark) systems. The investigation of such reactions makes it possible to study the two- and, perhaps, three-particle structure functions.

(2) Study of spin effects in reactions with large transfers, particularly in reactions involving polarized deuterons.

(3) Study of muon-pair production in collisions of relativistic nuclei and the hadron accompaniment of muon pairs.

(4) Study of the dynamics of particle multiple-production processes on the basis of measurements of the correlation function and the azimuthal correlations in particle production on light and heavy nuclei for the purpose of isolating the "elementary event" corresponding to a local interaction.

(5) Study of the x dependence of the nuclear structure functions separately for valence and sea quarks in the cumulative and noncumulative kinematics of muon-pair production. By measuring the isotopic content of the fragmenting nuclei (the proton and neutron content), it is possible to obtain data on the x distribution of the sea separately for the proton and the neutron.

In addition, there are plans to continue the studies using the internal target of the nuclotron, which allows investigation of the region of the transition from the nucleon degrees of freedom of nuclei to the quark–gluon degrees of freedom as the initial beam energy changes. These problems and the possibilities offered by the accelerator complex at the JINR High Energy Physics Laboratory are discussed in considerable detail in Refs. 108 and 109.

The present work was performed at the JINR High Energy Physics Laboratory, where studies in relativistic nuclear physics were initiated. I am deeply grateful to Academician A. M. Baldin, who laid the foundations for research in this area and continues to actively support it.

The operation of the installation in synchrophasotron beams, the data collection, and the processing and analysis of the experimental results involved my colleagues G. S. Averichev, N. Giordenescu, P. I. Zarubin, O. Yu. Kul'pina, N. S. Moroz, Yu. A. Panebrattsev, M. Pentsya, V. G. Perevozchikov, and A. N. Khrenov. I am deeply grateful to all of them. I would like to give special thanks to A. G. Litvinenko for numerous and fruitful discussions of the ques-

tions which arose in the course of the work. I am always grateful to now-deceased Prof. V. S. Stavinskiĭ, who possessed a clear understanding of all the problems discussed here and was always ready to share his knowledge.

Finally, I would like to express my deep thanks to A. I. Malakhov for his great and varied help throughout this work. I am also indebted to my colleagues in the SPHERE collaboration Yu. S. Anisimov, S. V. Afanas'ev, A. Yu. Isupov, V. I. Kolesnikov, G. L. Melkumov, I. I. Migulin, S. G. Reznikov, and A. Yu. Semenov.

This work was performed with the support of the Russian Fund for Fundamental Research, Grants 95-02-050070 and 96-02-17207.

APPENDIX

Here we present the tabulated data on the invariant differential cross sections for the processes that we have studied in the form

$$\frac{1}{A}E\frac{d\omega}{d\mathbf{p}}=\frac{1}{A}\frac{E}{p^2}\frac{d^2\sigma}{dpd\Omega}\ (\text{mb}\cdot\text{GeV}^{-2}\cdot\text{sec}^3\cdot\text{sr}^{-1}\cdot\text{nucleon}^{-1}).$$

Tables IX–XII contain the data on the A dependence of the cross sections for beams of protons, deuterons, helium, and carbon with momentum per nucleon equal to 4.5 GeV/c. In Table XIII we give the cross sections for K^+-meson production in the same beams. Next we give the data obtained using an 8.9-GeV/c proton beam. Table XIV contains the data on the A dependence of the cross sections of 0.5-GeV/c K^+ and K^- mesons. The energy dependence of the cross sections in the momentum range 0.3–0.7 GeV/c is given in Tables XV–XIX. The parameters of the approximations of the proton, pion, and deuteron cross sections in various representations are given in Tables XX–XXXVII.

[1)]The author is grateful to S. B. Gerasimov for a discussion of this topic.

[1] A. M. Baldin, Kratk. Soobshch. Fiz., No. 1, 35 (1971) [in Russian].
[2] A. M. Baldin *et al.*, Preprint R1-5819, JINR, Dubna (1971) [in Russian].
[3] J. Benecke *et al.*, Phys. Rev. **188**, 2159 (1969).
[4] G. A. Leksin, Zh. Éksp. Teor. Fiz. **32**, 445 (1957) [Sov. Phys. JETP **5**, 378 (1957)].
[5] L. S. Azhgireĭ *et al.*, Zh. Éksp. Teor. Fiz. **33**, 1185 (1957) [Sov. Phys. JETP **6**, 911 (1958)].
[6] D. I. Blokhintsev, Zh. Éksp. Teor. Fiz. **33**, 1295 (1957) [Sov. Phys. JETP **6**, 995 (1958)].
[7] A. M. Baldin, Fiz. Élem. Chastits At. Yadra **8**, 429 (1977) [Sov. J. Part. Nucl. **8**, 175 (1977)].
[8] V. S. Stavinskiĭ, Fiz. Élem. Chastits At. Yadra **10**, 949 (1979) [Sov. J. Part. Nucl. **10**, 373 (1979)].
[9] V. K. Luk'yanov and A. I. Titov, Fiz. Élem. Chastits At. Yadra **10**, 815 (1979) [Sov. J. Part. Nucl. **10**, 321 (1979)].
[10] M. I. Strikman and L. L. Frankfurt, Fiz. Élem. Chastits At. Yadra **11**, 571 (1980) [Sov. J. Part. Nucl. **11**, 221 (1980)].
[11] A. V. Efremov, Fiz. Élem. Chastits At. Yadra **13**, 613 (1982) [Sov. J. Part. Nucl. **13**, 254 (1982)].
[12] A. M. Baldin *et al.*, Yad. Fiz. **18**, 79 (1973) [Sov. J. Nucl. Phys. **18**, 41 (1974)].
[13] A. M. Baldin *et al.*, Yad. Fiz. **20**, 1201 (1974) [Sov. J. Nucl. Phys. **20**, 629 (1975)].
[14] A. M. Baldin *et al.*, Preprint E1-82-472, JINR, Dubna (1982).
[15] A. M. Baldin *et al.*, Preprint R1-83-432, JINR, Dubna (1983) [in Russian].
[16] Y. D. Bayukov *et al.*, Phys. Rev. C **20**, 764 (1979).
[17] S. Frankel *et al.*, Phys. Rev. C **20**, 2257 (1979).
[18] N. A. Nikiforov *et al.*, Phys. Rev. C **22**, 700 (1980).
[19] S. V. Boyarinov *et al.*, Yad. Fiz. **46**, 1472 (1987) [Sov. J. Nucl. Phys. **46**, 871 (1987)].
[20] S. V. Boyarinov *et al.*, Yad. Fiz. **50**, 1605 (1989) [Sov. J. Nucl. Phys. **50**, 996 (1989)].
[21] S. V. Boyarinov *et al.*, Yad. Fiz. **54**, 119 (1991) [Sov. J. Nucl. Phys. **54**, 71 (1991)].
[22] S. V. Boyarinov *et al.*, Yad. Fiz. **56**, No. 1, 125 (1993) [Phys. At. Nucl. **56**, 72 (1993)].
[23] O. P. Gavrishchuk *et al.*, Nucl. Phys. **A523**, 589 (1991).
[24] I. M. Belyaev *et al.*, Yad. Fiz. **56**, No. 10, 135 (1993) [Phys. At. Nucl. **56**, 1378 (1993)].
[25] Yu. M. Antipov *et al.*, Yad. Fiz. **53**, 439 (1991) [Sov. J. Nucl. Phys. **53**, 274 (1991)].
[26] G. A. Leksin, in *Some Problems in Experimental High-Energy Physics* [in Russian] (Moscow Engineering Physics Institute, Moscow, 1975).
[27] G. A. Leksin, in *Proc. of the Eighteenth Intern. Conf. on High-Energy Physics* [in Russian], Dubna, 1977, Vol. 1, A6-3.
[28] A. M. Baldin, in *Proc. of the Intern. Conf. on Extreme States in Nuclear Systems*, Dresden, 1980, Vol. 2, p. 1.
[29] A. M. Baldin *et al.*, in *Proc. of the Fourth Intern. Seminar on Problems in High-Energy Physics* [in Russian], Dubna, 1975, Report D1,2-9224, p. 176.
[30] A. M. Baldin *et al.*, Preprint R1-11302, JINR, Dubna (1978) [in Russian].
[31] L. S. Vorob'ev *et al.*, Yad. Fiz. **44**, 1396 (1986) [Sov. J. Nucl. Phys. **44**, 908 (1986)].
[32] Yu. D. Bayukov *et al.*, Preprint ITEP-76, ITEP, Moscow (1980) [in Russian].
[33] M. S. Kozodaev and A. A. Tyapkin, Prib. Tekh. Éksp. **1**, 21 (1956) [in Russian].
[34] T. V. Avericheva *et al.*, Preprint 1-11317, JINR, Dubna (1978) [in Russian].
[35] A. M. Baldin *et al.*, Preprint R1-83-433, JINR, Dubna (1983) [in Russian].
[36] A. M. Baldin *et al.*, Preprint R1-83-434, JINR, Dubna (1983) [in Russian].
[37] G. S. Averichev *et al.*, in *Proc. of the Tenth Intern. Seminar on High Energy Physics Problems* (World Scientific, Singapore, 1991), p. 90.
[38] A. Bohr and B. R. Mottelson, *Nuclear Structure*, Vol. 1 (Benjamin, New York, 1969) [Russ. transl., Mir, Moscow, 1971].
[39] V. K. Bondarev *et al.*, in *Relativistic Nuclear Physics and Quantum Chromodynamics*, edited by A. M. Baldin and V. V. Burov (Dubna, 1994), p. 235.
[40] H. de Vries *et al.*, At. Data Nucl. Data Tables **36**, 496 (1987).
[41] V. K. Bondarev *et al.*, Preprint E1-93-84, JINR, Dubna (1993).
[42] V. K. Bondarev, in *Proc. of the Conf. Hadron Structure '94*, Košice, Slovakia, 1994, edited by J. Urbán and J. Vrláková, p. 177.
[43] A. M. Baldin *et al.*, Preprint 1-82-28, JINR, Dubna (1982) [in Russian].
[44] M. I. Strikman and L. L. Frankfurt, Yad. Fiz. **32**, 1403 (1980) [Sov. J. Nucl. Phys. **32**, 725 (1980)].
[45] V. B. Gavrilov *et al.*, Preprint ITEP-121, ITEP, Moscow (1985) [in Russian].
[46] V. K. Bondarev *et al.*, in *Proc. of the Eighth Intern. Seminar on Problems in High-Energy Physics* [in Russian], Dubna, 1986, Report D1,2-86-668, p. 243.
[47] A. M. Baldin *et al.*, Yad. Fiz. **21**, 1008 (1975) [Sov. J. Nucl. Phys. **21**, 517 (1975)].
[48] V. K. Bondarev *et al.*, JINR Rapid Commun. 1(58)-93, p. 53, JINR, Dubna (1993).
[49] Yu. D. Bayukov *et al.*, Preprint ITEP-148, ITEP, Moscow (1983) [in Russian].
[50] A. M. Baldin, Preprint E2-83-415, JINR, Dubna (1983).
[51] A. M. Baldin *et al.*, in *Multiquark Interactions and Quantum Chromodynamics* [in Russian], Dubna, 1984, Report D1,2-84-599, p. 195.
[52] A. M. Baldin *et al.*, in *Proc. of the Second Intern. Conf. on Nucleus–Nucleus Collisions*, Visby, Sweden, 1985, edited by B. Jakobsson and K. Aleklett, Vol. 1, p. 75.
[53] A. A. Logunov *et al.*, Fiz. Élem. Chastits At. Yadra **14**, 493 (1983) [Sov. J. Part. Nucl. **14**, 201 (1983)].
[54] I. A. Savin and G. I. Smirnov, Fiz. Élem. Chastits At. Yadra **22**, 1005 (1991) [Sov. J. Part. Nucl. **22**, 489 (1991)].
[55] A. C. Benvenuti *et al.* (BCDMS Collaboration), Preprint E1-93-133, JINR, Dubna (1993) [submitted to Nucl. Phys. A].

[56] P. Amaudruz *et al.*, Preprint CERN-PPE/91-47, CERN, Geneva (1991); Z. Phys. C **53**, 73 (1992).
[57] R. Hofstadter *et al.*, in *The Electromagnetic Structure of Nuclei and Nucleons* [in Russian] (IL, Moscow, 1958).
[58] Yu. D. Bayukov *et al.*, Preprint ITEP-8, ITEP, Moscow (1983) [in Russian].
[59] M. Kh. Anikina *et al.*, Preprint R1-85-208, JINR, Dubna (1985) [in Russian].
[60] G. N. Agakishiev *et al.*, Preprint R1-89-793, JINR, Dubna (1989) [in Russian].
[61] A. G. Litvinenko *et al.*, JINR Rapid Commun. 1(58)-93, p. 27, JINR, Dubna (1993).
[62] K. V. Alanakyan *et al.*, Yad. Fiz. **25**, 545 (1977) [Sov. J. Nucl. Phys. **25**, 292 (1977)].
[63] R. Ammar *et al.*, Preprint FIAN-48, Lebedev Physics Institute, Moscow (1988) [in Russian].
[64] R. Ammar *et al.*, Pis'ma Zh. Éksp. Teor. Fiz. **49**, 189 (1989) [JETP Lett. **49**, 219 (1989)].
[65] Yu. D. Bayukov *et al.*, Yad. Fiz. **41**, 158 (1985) [Sov. J. Nucl. Phys. **41**, 101 (1985)].
[66] L. S. Schroeder *et al.*, Phys. Rev. Lett. **43**, 1787 (1979).
[67] S. B. Gerasimov *et al.*, Preprint R2-7687, JINR, Dubna (1974) [in Russian].
[68] V. V. Burov *et al.*, Preprint R2-10244, JINR, Dubna (1976) [in Russian].
[69] S. V. Afanasiev *et al.*, Phys. Scr. **48**, 124 (1993).
[70] E. Moeller *et al.*, Phys. Rev. C **28**, 1246 (1983).
[71] V. B. Kopeliovich, Yad. Fiz. **26**, 168 (1977) [Sov. J. Nucl. Phys. **26**, 87 (1977)].
[72] E. N. Bol'nin, in *Proc. of the Eighteenth Winter School of the Leningrad Nuclear Physics Institute* [in Russian], p. 63 (Leningrad, 1983).
[73] I. M. Belyaev *et al.*, Preprint R1-89-463, JINR, Dubna (1989) [in Russian].
[74] M. A. Braun and V. V. Vechernin, Yad. Fiz. **25**, 1276 (1977) [Sov. J. Nucl. Phys. **25**, 676 (1977)].
[75] A. V. Efremov, Yad. Fiz. **24**, 1208 (1976) [Sov. J. Nucl. Phys. **24**, 633 (1976)].
[76] J. W. Cronin *et al.*, Phys. Rev. D **11**, 3105 (1975).
[77] G. Berlad *et al.*, Phys. Rev. D **22**, 1547 (1980).
[78] M. I. Strikman and L. L. Frankfurt, Pis'ma Zh. Éksp. Teor. Fiz. **30**, 373 (1979) [JETP Lett. **30**, 346 (1979)].
[79] L. L. Frankfurt and M. I. Strikman, Phys. Lett. **83B**, 407 (1979).
[80] L. L. Frankfurt and M. I. Strikman, Phys. Rep. **76**, 215 (1981).
[81] L. L. Frankfurt and M. I. Strikman, Phys. Rep. **160**, 235 (1988).
[82] M. A. Braun, Yad. Fiz. **48**, 409 (1988) [Sov. J. Nucl. Phys. **48**, 257 (1988)].
[83] M. A. Braun and V. V. Vechernin, Yad. Fiz. **51**, 873 (1990) [Sov. J. Nucl. Phys. **51**, 555 (1990)].
[84] V. B. Gavrilov *et al.*, Yad. Fiz. **41**, 843 (1985) [Sov. J. Nucl. Phys. **41**, 540 (1985)].
[85] M. A. Braun and V. V. Vechernin, in *Relativistic Nuclear Physics and Quantum Chromodynamics*, edited by A. M. Baldin and V. V. Burov, Dubna, 1994, p. 294.
[86] A. M. Baldin *et al.*, in *Multiquark Interactions and Quantum Chromodynamics* [in Russian], Dubna, 1984, Report D1,2-84-599, p. 195.
[87] V. S. Stavinskiĭ, in *Relativistic Nuclear Physics and Quantum Chromodynamics* [in Russian], Dubna, 1988, Report D1,2-88-652, p. 190.
[88] M. I. Gorenstein and G. M. Zinovjev, Phys. Lett. **67B**, 100 (1977).
[89] M. I. Gorenshteĭn *et al.*, Yad. Fiz. **26**, 788 (1977) [Sov. J. Nucl. Phys. **26**, 414 (1977)].
[90] I. G. Bogatskaya *et al.*, Yad. Fiz. **27**, 856 (1978) [Sov. J. Nucl. Phys. **27**, 454 (1978)].
[91] I. G. Bogatskaya *et al.*, Phys. Rev. C **22**, 209 (1980).
[92] D. V. Anchishkin *et al.*, Preprint ITP-81-75E, ITP, Kiev (1981).
[93] A. V. Efremov, Yad. Fiz. **44**, 776 (1986) [Sov. J. Nucl. Phys. **44**, 501 (1986)].
[94] A. V. Efremov, Preprint R2-87-762, JINR, Dubna (1987) [in Russian].
[95] A. V. Efremov *et al.*, Yad. Fiz. **47**, 1364 (1988) [Sov. J. Nucl. Phys. **47**, 868 (1988)].
[96] A. V. Efremov *et al.*, Preprint E2-93-224, JINR, Dubna (1993).
[97] A. V. Efremov *et al.*, in *Relativistic Nuclear Physics and Quantum Chromodynamics*, edited by A. M. Baldin and V. V. Burov, Dubna, 1994, p. 309.
[98] A. M. Baldin, in *Proc. of the Second Intern. Conf. on Nucleus–Nucleus Collisions*, Visby, Sweden, 1985, edited by B. Jakobsson and K. Aleklett, Vol. 1, p. 73.
[99] Yu. É. Penionzhkevich, Fiz. Élem. Chastits At. Yadra **25**, 930 (1994) [Phys. Part. Nucl. **25**, 394 (1994)].
[100] A. V. Vlasov *et al.*, Preprint ITEP-57-90, ITEP, Moscow (1990) [in Russian]; Yad. Fiz. **58**, 669 (1995) [Phys. At. Nucl. **58**, 613 (1995)].
[101] A. M. Baldin and L. A. Didenko, Kratk. Soobshch. JINR No. 3-84, p. 5, Dubna (1984) [in Russian].
[102] A. M. Baldin and L. A. Didenko, Kratk. Soobshch. JINR No. 8-85, p. 5, Dubna (1985) [in Russian].
[103] D. Armutliĭski, A. M. Baldin *et al.*, Kratk. Soobshch. JINR No. 4[24]-87, p. 5, Dubna (1987) [in Russian].
[104] A. M. Baldin *et al.*, Preprint R1-88-331, JINR, Dubna (1988) [in Russian].
[105] J. Bartke, Int. J. Mod. Phys. A **4**, 1319 (1989).
[106] A. M. Baldin *et al.*, Yad. Fiz. **52**, 1427 (1990) [Sov. J. Nucl. Phys. **52**, 903 (1990)].
[107] A. M. Baldin and L. A. Didenko, Fortschr. Phys. **38**, 261 (1990).
[108] S. A. Averichev *et al.*, Preprint R1-85-512, JINR, Dubna (1985) [in Russian].
[109] A. M. Baldin and A. I. Malakhov, JINR Rapid Commun. No. 3[60]-93, p. 52, Dubna (1993).
[110] A. M. Baldin, in *Relativistic Nuclear Physics and Quantum Chromodynamics*, edited by A. M. Baldin and V. V. Burov, Dubna, 1994, p. 672.

Translated by Patricia A. Millard